Journal of Hydrology 608 (2022) 127545

Contents lists available at ScienceDirect

Journal of Hydrology

journal homepage: www.elsevier.com/locate/jhydrol

Research papers

Diagnosing changes in glacier hydrology from physical principles using a hydrological model with snow redistribution, sublimation, firnification and energy balance ablation algorithms

Dhiraj Pradhananga [a,b,c,*], John W. Pomeroy [a]

[a] Centre for Hydrology, University of Saskatchewan, Canmore, 1151 Sidney Street, Alberta T1W 3G1, Canada
[b] Department of Meteorology, Tri-Chandra Multiple Campus, Tribhuvan University, Kathmandu, Nepal
[c] The Small Earth Nepal, P.O. Box 20533, Kathmandu, Nepal

ARTICLE INFO

This manuscript was handled by Marco Borga, Editor-in-Chief, with the assistance of Francesco Avanzi, Associate Editor"

Keywords:
Glacier hydrology
Energy-budget melt
Mass balance
Snow redistribution
Peyto Glacier
Athabasca Glacier
Hydrological modelling

ABSTRACT

A comprehensive glacier hydrology model was developed within the Cold Regions Hydrological Modelling platform (CRHM) to include modules representing wind flow over complex terrain, blowing snow redistribution and sublimation by wind, snow redistribution by avalanches, solar irradiance to sloping surfaces, surface sublimation, glacier mass balance and runoff, meltwater and streamflow routing. The physically based glacier hydrology model created from these modules in CRHM was applied to simulate the hydrology of the instrumented, glacierized and rapidly deglaciating Peyto and Athabasca glacier research basins in the Canadian Rockies without calibration of parameters from streamflow. It was tested against observed albedo, point and aggregated glacier mass balance, and streamflow and found to successfully simulate surface albedo, snow redistribution, snow and glacier accumulation and ablation, mass balance and streamflow discharge, both when driven by in-situ observations and reanalysis forcing data. Long term modelling results indicate that the increases in discharge from the 1960s to the present are due to increased glacier ice melt contributions, despite declining precipitation and snow melt.

1. Introduction

Changes in alpine snow and glacier hydrology influence both timing and magnitude of streamflow discharge, and thus impact the water supply for downstream industrial, agricultural, hydropower, environmental and drinking purposes around the world. These changes include the rapid retreat of glaciers (Arendt et al., 2009; Berthier, 2004; Demuth and Pietroniro, 2003; Diolaiuti et al., 2011; Fujita and Nuimura, 2011; Haeberli et al., 2007; Kaser et al., 2004; Naz et al., 2014; Ohmura, 2006; Schiefer et al., 2007), declining seasonal snowcover at higher elevations (Fujita and Nuimura, 2011; IPCC, 2007; Mote et al., 2005), and declining streamflow (Demuth and Pietroniro, 2003; Immerzeel et al., 2010; Kienzle et al., 2012; Rood et al., 2008). In particular, the influence of glacier snow and ice melt dominates the seasonal pattern of runoff in mid to high latitude mountains more than low latitude high mountains (Kaser et al., 2003).

The Canadian Rockies constitute the headwaters of the major rivers of western Canada and northwest US; for example, the Saskatchewan-Nelson, Columbia, Fraser, and Columbia rivers. Snow and ice in these mountain headwaters regulate the hydrology of the rivers by acting as a short to long term water storage reservoir (López-Moreno et al., 2020). But North American mountain glaciers are retreating (Arendt et al., 2002; Berthier, 2004; Berthier et al., 2010; Comeau et al., 2009; DeBeer et al., 2007; Demuth and Pietroniro, 2003; Moore and Demuth, 2001; Munro, 2000; Schiefer et al., 2007) thus causing changes to this reservoir function. Observations suggest that there is a pronounced acceleration in the glacier retreat in the Canadian Rockies (Moore et al., 2009), which is very noticeable in the case of Peyto Glacier (e.g., Demuth and Keller, 2006; Kehrl et al., 2014). Changes in North American glacier mass, area, and shape result in changing contributions to water resources (Barry, 2006; Reynolds and Young, 1997), and these changes in glacier elevation and volume are related to changes in temperature and precipitation (Tennant and Menounos, 2013). The other notable change in most glaciers is the rise in their equilibrium line altitudes (ELA) due to warming climate (Malecki, 2015; Van Pelt and Kohler, 2015; Zemp et al., 2015). The ELA is the dividing elevation between accumulation

* Corresponding author at: Centre for Hydrology, University of Saskatchewan, Canmore, 1151 Sidney Street, Alberta T1W 3G1, Canada.
E-mail addresses: dhiraj.pradhananga@usask.ca (D. Pradhananga), john.pomeroy@usask.ca (J.W. Pomeroy).

https://doi.org/10.1016/j.jhydrol.2022.127545
Received 28 June 2021; Received in revised form 21 January 2022; Accepted 25 January 2022
Available online 2 February 2022

and ablation zones on a mountain glacier and so its elevation indexes the glacier mass balance. Variations in the ELA are commonly attributed to changes of winter precipitation and summer air temperature (Bakke and Nesje, 2011). Therefore, there are changes in glacier mass, ELA and in streamflow. It is essential to understand how the decline of alpine snowcover and glacier mass in the mountains is influencing streamflow generation, as this can help to predict the availability of future water resources.

Snow and glacier melt models range from complex energy budget models (Hock and Holmgren, 2005; Klok et al., 2002; Magnusson et al., 2010; Michlmayr et al., 2008; Mott et al., 2008; Munro, 2011a; Munro, 2004; Munro and Marosz-Wantuch, 2009; Naz et al., 2014; Oerlemans, 1991; Shea et al., 2015) to more simplified degree-day models (Anderson et al., 2006; Hock, 1999; Immerzeel et al., 2012). Most glacier hydrology models use simple conceptual melt models that are based on temperature and precipitation observations and are calibrated from past conditions (see Hock, 2005 for review). Examples include statistical and temperature index models (Fujita and Nuimura, 2011; Hannah and Gurnell, 2001; Hock, 2003, 1999; Luo et al., 2013; Shea and Marshall, 2007; Singh and Bengtsson, 2005; Stahl et al., 2008; Verbunt et al., 2003). These empirical models do not consider the redistribution of snow by wind and avalanches, sublimation losses, and the full radiation energetics that are critical to the survival of small mountain glaciers (Déry et al., 2010). Because high altitude observations of shortwave irradiance are limited, empirical techniques that rely upon commonly measured variables, such as air temperature, have led to the popularity of the temperature-index model and its wide use to simulate glacier snow and ice melt (Hock, 2005). These empirical methods are unlikely to be reliable for future conditions, as they have been calibrated based on past climates (Poulin et al., 2011). Walter et al. (2005), however, demonstrated that a physically based energy budget melt model does not require more input data than most temperature-index methods or what is available on most modern meteorological stations. The Energy Budget Snowmelt Model (EBSM) of Gray and Landine (1988) is an example of such a physically based snow model that only requires precipitation, temperature, humidity and wind speed information. Pomeroy et al. (2013) showed that shortwave and net radiation can be synthesized from temperature and humidity data to drive energy budget snowmelt and evapotranspiration algorithms. For example, several relationships have been developed to estimate shortwave (Shook and Pomeroy, 2011) and longwave radiation (Sicart et al., 2006) from latitude, time of year, air temperature, and vapour pressure. Sicart et al. (2006) evaluated longwave and shortwave radiation estimates from these methods over mountain (Wolf Creek Research Basin in Yukon Territory) and prairie (Saskatchewan) sites in Canada and found that simulated values were close to measurements. Moreover, reanalysis products are now commonly being used to force hydrological models (Krogh et al., 2015) making application of the energy balance more straightforward than in the past.

The Cold Regions Hydrological Modelling platform (CRHM, Pomeroy et al., 2007) is a flexible, object-oriented, process-based modelling platform that runs on spatially distributed hydrological response units (HRU) at sub-daily or sub-hourly timesteps. HRU are landscape units having a common set of parameters and modules and that have some common biogeophysical and drainage characteristics. HRU are used to distribute meteorological forcing data over the basin and in this application are based on slope, aspect, elevation and landcover type, including glacier coverage. CRHM simulates several cold region hydrological processes that are important in high mountain environments such as blowing snow redistribution, blowing snow sublimation, infiltration into frozen soils, radiation exchange in complex terrain, snow accumulation and ablation, as well as the full range of hydrological processes for warm seasons such as evapotranspiration, infiltration, soil moisture movement, groundwater dynamics, surface runoff and interflow (Pomeroy et al., 2007; Fang et al., 2013). The model runs through interactions of the four components - observations, parameters, modules, and state variables through calculation of mass and energy budgets on the HRU, sub-basin and basin levels of discretization. Blowing snow, avalanches, runoff, interflow and groundwater flow can move via various pathways from HRU to HRU(s) and streamflow is routed from various sub-basins to the basin outlet. Through these interactions, CRHM links atmospheric data inputs and hydrological outputs. The minimum atmospheric inputs required to force CRHM are air temperature, humidity, wind speed and precipitation either from automatic weather stations or from atmospheric model outputs for the surface level. CRHM has been successfully applied to many regions, ranging from the Canadian Prairies to high mountains in North and South America (Ellis et al., 2010; Fang et al., 2010; Fang and Pomeroy, 2007; Krogh et al., 2015; Lv and Pomeroy, 2019; MacDonald et al., 2010, 2009; Rasouli et al., 2014), Europe (López-Moreno et al., 2013), Africa (López-Moreno et al., 2020) and Asia (Zhou et al., 2014).

Recent research has coupled basin hydrology modelling with glacier dynamics to assess the impact of glacier retreat on streamflow (Finger et al., 2013; Huss, 2011; Huss et al., 2005; Immerzeel et al., 2012; Naz et al., 2014; Shea et al., 2015). However, these and other studies have not considered many of the important cold region hydrological processes, including the evolution, ablation and redistribution of snow. Snow storage, redistribution of snow by wind and gravity, and sublimation rates in high latitude alpine mountains are crucial processes to consider when determining meltwater contribution to the basin (Ayala Ramos, 2017; Bernhardt and Schulz, 2010; Bravo et al., 2017; MacDonald et al., 2010; Strasser et al., 2008). Despite significant advances in the understanding of blowing snow redistribution and sublimation processes (Déry et al., 2010; Doorschot et al., 2001; Essery and Pomeroy, 2004; Liston and Elder, 2006; MacDonald et al., 2009; Pomeroy and Li, 2000), they have not yet been included in mountain glacier melt studies in the Canadian Rockies. They have been considered in mass balance and melt studies over Icelandic and polar glaciers (Déry et al., 2004), as well as in studies of Greenland (Mernild et al., 2008; Mernild et al., 2007), Antarctic (Bintanja and Reijmer, 2001; Gallée et al., 2012; Thiery et al., 2012) and Arctic (Bintanja, 2001; Liston and Hiemstra, 2011) sea ice and ice-sheets.

These studies suggest snow redistribution, snow sublimation and other hydrological processes may also contribute to the mass and energy budgets of mountain glaciers in western Canada. Therefore, there is a need to develop a glacial melt model that utilizes an energy budget approach, physically measurable inputs, and a snow redistribution approach that accounts for the complex mass transport present in mountainous regions. It is hypothesized that the simulation of water contributions from glacial ablation will be more accurate when snow redistribution by wind and gravity, sublimation and surface energy budget energetics are included. This study develops and tests a comprehensive physically based and spatially distributed model of glacier snow and ice hydrology at two glacierized research basins in the Canadian Rockies. The CRHM-glacier model, developed within CHRM, includes redistribution of snow by wind and avalanches, an energy budget melt model for snow, firn and ice, consideration of slope and aspect for radiation distribution, and runoff routing.

2. Study sites and data

2.1. Two instrumented, partially glacierized, alpine basins in the Canadian Rockies

Peyto Glacier Research Basin (PGRB, Latitude: $51^0$40′N and Longitude: $116^0$33′W) in Banff National Park and Athabasca Glacier Research Basin (AGRB, Latitude: $52^0$11′N and Longitude: $117^0$16′W) in Jasper National Park, both in Alberta, Canada, were considered for testing the CRHM-glacier model (Figs. 1 and 2). Both research sites are part of the Canadian Rockies Hydrological Observatory – a network of instrumented basins in the mountain headwaters of the Saskatchewan and Athabasca River basins operated by the University of Saskatchewan

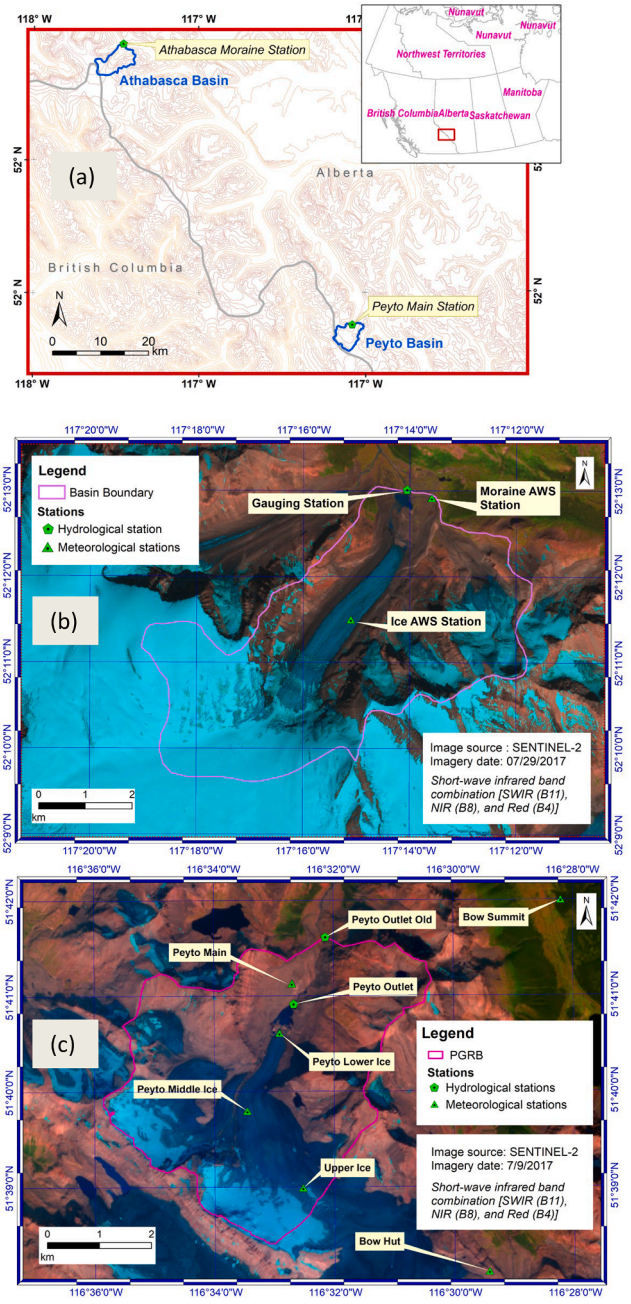

Figure 1: (a) Location of Peyto and Athabasca glacier research basins ir

Fig. 1. (a) Location of Peyto and Athabasca glacier research basins in Western Canada; (b) AGRB and location of hydrometeorological stations; (c) PGRB and location of hydrometeorological stations within and nearby the basin.

Centre for Hydrology. PGRB, with its outlet at the former streamflow gauging site (Peyto Outlet Old, Fig. 1 (c)), covers an area of 22.43 km^2, which included 9.9 km^2 of glacierized area as of 2016. AGRB has a basin area of 29.3 km^2 including 16.9 km^2 of glacierized area in 2016. Peyto Glacier in PGRB is a valley outflow glacier of the Wapta Icefield in the Waputik Mountains. Athabasca Glacier in AGRB is a valley outflow glacier of the Columbia Icefield. Streamflow out of PGRB flows east into the Mistaya River Basin, a headwater of the North Saskatchewan River and eventually into the Hudson Bay via the Nelson River; and that out of AGRB flows north through the Sunwapta River, a headwater of the Athabasca River and eventually into the Beaufort Sea of the Arctic Ocean via the Mackenzie River. Table 1 provides the general physical characteristics of these two research basins. These basins were equipped in

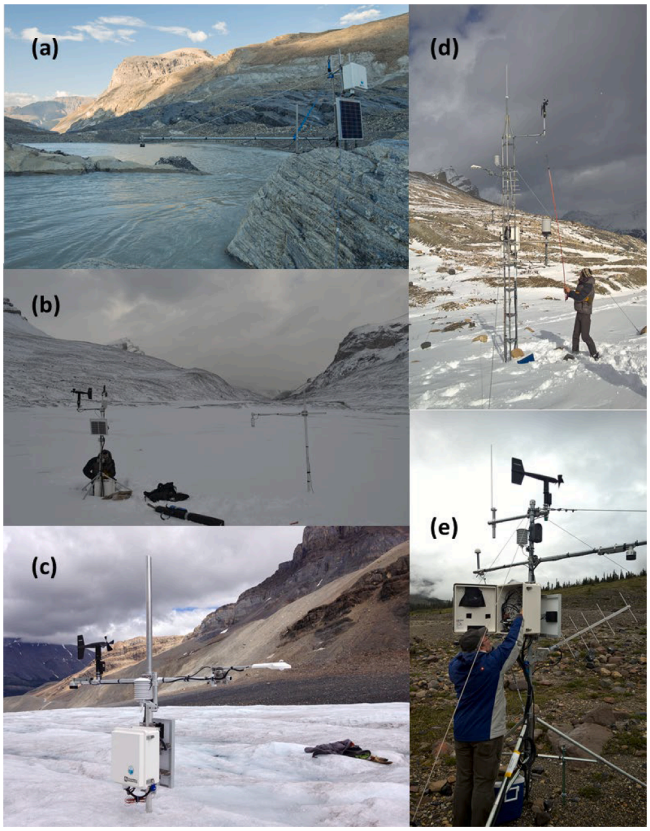

Fig. 2. AWSs in AGRB and PGRB. (a) New gauging station at the outlet of Munro Lake, (b) Peyto Lower Ice station (c) Athabasca Ice station, (d) Peyto Main station, (e) Athabasca Moraine station. [Photo (a) by May Guan; the rest by Dhiraj Pradhananga]

Table 1
Physical characteristics of the study basins.

Basin configuration	PGRB	AGRB
Basin area	22.4 km^2	29.3 km^2
Glacier area	9.9 km^2 [44%] as of 2016	16.9 km^2 [58%] as of 2016
Elevation range of basin	1907 – 3152 m as of 2014	1926 – 3459 m as of 2011
Location	51^{0}40′N, 116^{0}33′W Banff National Park, Alberta	52^{0}11′N, 117^{0}16′W Jasper National Park, Alberta
Mean elevation of glacier	2615 m [2014 DEM, 2016 Landcover]	2826 m [2011 DEM, 2016 Landcover]
Basin outlets	Old gauge: 51°41′37″N; 116°32′08″W New gauge: 51°40′52″N; 116°32′41″W	52°12′58″N; 117°13′55″W

2013–2014 with new automatic weather stations (AWS) on-ice and off-ice sites. The instrumentation and range of parameters measured at these AWS are presented in Table 2.

These glaciers have been losing mass continuously since the mid-1970 s (Demuth and Keller, 2006; Kehrl et al., 2014; Tennant and Menounos, 2013). In the case of Peyto Glacier, a new proglacial lake, "Lake Munro", formed at the tongue of the glacier and is increasing in size every year. Peyto Creek, flowing out of Lake Munro, drains the meltwater from the glacier and discharges to Peyto Lake, which has outflow into the Mistaya River. The first record of Peyto Glacier goes back to 1897 (photograph by Walter D. Wilcox) and it was subject to intermittent scientific investigations in the 1930s, 1940s and 1950s. Significant research over the glacier started in 1965 when it was selected

Table 2
Instrumentation and parameters measured at AWS in the study basins.

Variable	Instrument	Units
Air temperature	Rotronic HC2-S3 Temperature and Humidity Probe	degree C
Relative humidity		%
Snow depth	SR50A Sonic Ranger	m
Wind speed	RM Young 05103-10 Wind Monitor	m s^{-1}
Wind direction	05103AP-10	degrees
Incoming shortwave radiation	Kipp & Zonen CNR4 Net Radiometer	W m^{-2}
Outgoing shortwave radiation		
Incoming longwave radiation		
Outgoing longwave radiation		
Barometric pressure	Vaisala CS106	hPa
Snow temperature	Omega Type E Thermocouple	degree C
Volumetric water content	Campbell Scientific CS650	%
Electroconductivity		dS m^{-1}
Soil temperature		degree C
Soil heat flux	HFP01	W m^{-2}
Rainfall	TB4 tipping bucket rain gauge	mm
Precipitation	Ott Pluvio	mm

as one of the research sites for the UNESCO International Hydrological Decade (IHD). The scientific scope and instruments used for observations have increased and improved progressively since then (Munro, 2013). As reported by Meek (1948), surveys documenting the recession and flow of Athabasca Glacier began in 1945.

2.2. Data

2.2.1. Topography

Several digital elevation models (DEM) from different years, topographical maps and satellite images were considered for both the basins. For PGRB, the 1966 DEM (10 m resolution) was developed from the scanned topographic map of Peyto Glacier produced from the aerial photographs from August 1966 (Sedgwick and Henoch, 1975). The same map was used for considering landcover for 1966 of the basin. The 2006 DEM (10 m resolution) was obtained from airborne LiDAR measurements (Demuth and Hopkinson, 2013). Since the aerial photograph didn't cover the whole PGRB, the northeastern corner of the basin was mosaiced with the 2014 DEM to fill in the missing part. The 2014 DEM was prepared at a 10 m resolution from aerial photogrammetry of Banff National Park by Geodesy Group Inc. taken during July and September 2014. PGRB landcover maps for 2006 and 2014 were prepared based upon Landsat 5 satellite images for 2006 and Landsat 8 for 2014. For AGRB, DEMs from 1983 (Canadian Digital Elevation Model, CDEM), 2000 (Canadian Digital Surface Model, CDSM) and 2011, all at 20 m horizontal resolution, were available. Landcover maps were generated from Landsat 5 and Landsat 8 top-of-atmosphere reflectance images, using Google Earth Engine. Landsat 5 images were used for the years 1984 and 2006, and Landsat 8 images were used for 2014. The images acquired for this study were taken between 15th July to 15th September in the respective years, with minimum or no cloud cover inside the basin boundaries. The DEM and landcover data are summarized in Table 3.

2.2.2. Glaciology and hydrology

Past studies of Peyto Glacier are well documented in the book 'Peyto Glacier: One Century of Science' edited by Demuth et al. (2006). The book also provides details of the mass balance data, along with hypsometry of the glacier. Long-term glacier mass balance records are available for Peyto Glacier from 1965, with a data gap in 1991–1992. Glaciological mass balance measurements using ablation stakes and snow pits have been taken continuously since the IHD period. Mass balance data for the 11 elevation bands are available in several publications (Demuth and Keller, 2006; Ommanney, 1987; Young and Stanley, 1976). Though winter (Bw) and summer (Bs) balance records are available until 1994, annual glacier net mass balance (Bn) data are available after 1994 (WGMS, 2020). Mass balance data for Athabasca Glacier were not available for this study.

PGRB streamflow was gauged during the IHD period and then discontinued in 1977. In the summer of 2013, the University of Saskatchewan Centre for Hydrology established a stream gauging site in the basin, about 1.5 km upstream from the site used in the IHD. Locations of old and new gauges are shown in Fig. 6. Discharge data from the IHD period are available for an 11-year period (1967–1977) and those from the recent period are available for 6 years (2013–2018). Discharge data from the outlet of Athabasca Glacier are available from 1948 to the present, with a data gap from 1997 to 2004. Historical streamflow discharge data from PGRB and AGRB and recent data for AGRB were obtained from the Environment and Climate Change Canada's Water Survey of Canada.

Table 3
DEM and landcover maps.

Research basin	Simulation period	DEM (source)	Landcover (source)	HRUs
AGRB	2014–2019	2011 (JAXA)*	2014 (Landsat 8, 9 August)*	90
	1980–1989 1967–1977	1983 (CDEM)	1984 (Landsat 5, 28 July)	
PGRB	2010–2019	2014 (Lidar)*	2014 (Landsat 8, 18 August)*	65
	2006–2009	2006 (Lidar)	2006 (Landsat 5, 28 August)	
	1967–1977	1966 (Topographic map)*	1966 (Topographic map, August)*	70

*These DEMs and landcover data were used in deriving HRUs for the basins. Two separate HRUs were prepared for PGRB considering two basin outlets.

2.2.3. Meteorological forcing datasets

AWSs (Fig. 2) were installed at on-ice and off-glacier sites in AGRB and PGRB by the University of Saskatchewan Centre for Hydrology in 2013–2014. Archived hourly meteorological observations from the AWS at the Peyto Glacier Main station were available from 1987 (Munro, 2011a; Munro, 2011b) along with periodical observations made on the ice since 2007 (Pradhananga et al., 2021). Precipitation data from the Canadian Rockies Hydrological Observatory station above nearby Helen Lake (https://research-groups.usask.ca/hydrology/data.php) and the three stations Bow Summit, Saskatchewan River Crossing, and Lake Louise of Environment and Climate Change Canada (http://climate.weather.gc.ca/) were used to estimate elevational gradients in precipitation following the approach by Fang et al. (2013). Monthly values of temperature lapse rates were obtained from observations at the four AWS stations (Fig. 1c) at different elevations on PGRB. These monthly values of gradients in precipitation and temperature were applied to PGRB and then transferred to AGRB.

Preparation of meteorological data to provide continuous datasets suitable for forcing a hydrology model presents several challenges at these sites. Meteorological data collection from alpine glacier basins is challenged by remoteness, difficulty in accessibility, severe weather and year-round cold conditions and many other difficulties. Higher winter snow accumulations can bury on-ice stations, and increasingly rapid summer melt can cause the meteorological station towers or tripods to tilt or fall. Rapid ice melt means that stations needed to be re-installed by drilling 5 m into the ice twice a year. Therefore, the AWS located within and near the basin were used to fill in gaps (details are in Pradhananga et al. (2021) for PGRB). Reanalysis data were used to run the model beyond the observation periods. For PGRB, the model was also tested with Lake Louise precipitation data for the model run period 1967–1977

as this was the only proximal station in existence at the time.

The ERA global reanalysis datasets, ERA Interim (Dee et al., 2011) and ERA-40 (Uppala et al., 2005) were first bias-corrected to a single point at the main AWS stations on AGRB and PGRB by comparing with the *in-situ* observations at these sites, or proximal sites when precipitation was corrected for wind undercatch. A quantile mapping technique was used for the bias corrections of air temperature, vapour pressure, wind speed, precipitation, incoming shortwave and longwave radiation with parameters individually calibrated for each month from corresponding data periods using the qmap package in R (Gudmundsson, 2016). For AGRB, ERA-Interim data were bias-corrected to the Athabasca Moraine Station, which had observed data from 2014 to 2019. Since there was not any observed data before 2014 for AGRB, ERA-40 data were bias-corrected using ERA-Interim data for the period of 1979–2002, similar to the approach of Krogh and Pomeroy (2018). For PGRB, ERA-Interim data were bias-corrected to Peyto Main station observations from 2013 to 2019, except for precipitation data, which were taken from the proximal and sheltered Bow Summit observations. ERA-40 data for PGRB were bias-corrected to the archived observation from the station for the common overlap period of 1987–2001. These bias-corrected reanalysis datasets and *in-situ* observations over PGRB are published in Pradhananga et al. (2021). Lake Louise precipitation data were also bias-corrected to Bow Summit by monthly quantile mapping.

Using these datasets to force CRHM has been discussed by Krogh et al. (2017) and Krogh et al. (2015) and involves creating continuous hourly fields of temperature, humidity, wind speed, shortwave irradiance and either hourly or daily precipitation. These data were distributed to the basin using algorithms and macros in CRHM (Pomeroy et al., 2007). CRHM's 'Observation module' adjusted temperature and precipitation with elevation of each HRU based on monthly lapse rates, the 'Radiation module' distributed global radiation to HRUs based on latitude, elevation, ground slope and azimuth. Incoming longwave radiation was distributed in CRHM based on air temperature, humidity and the HRU terrain view factor. Wind speed acceleration and deceleration due to flow over complex terrain was adjusted using the Walmsley's parametric boundary layer wind flow module in CRHM (Walmsley et al., 1989). Details of these modules are provided by Fang et al. (2013). The model input data files were prepared using several R packages; CRHMr (Shook, 2016a) for pre-processing meteorological station forcing data, post-processing and analysing model outputs, MSCr (Shook, 2015) for pre-processing archived data from Environment and Climate Change Canada, and Reanalysis (Shook, 2016b) for pre-processing and interpolating atmospheric model reanalysis data.

3. CRHM-glacier

Glacier snow and ice energy and mass budgets and meltwater routing processes were incorporated into CRHM to create CRHM-glacier, a model suitable for alpine glacierized basins. These modules are linked in a sequential manner to simulate hydrological processes for a glacierized basin, following the flow diagram shown in Fig. 3. The most relevant modules for an alpine glacier dominated basin are described in the following subsections along with the new glacier module. This section also details the development of the distributed, physically based, numerical model to simulate glacier mass and energy fluxes.

3.1. Snow redistribution and sublimation

Many mountain glacier models neglect blowing snow and sublimation despite the prominence of these processes at high altitudes (e.g., Naz et al., 2014; Shea et al., 2015) and demonstration of improvements in model performance when these processes are included in alpine simulations (Fang et al., 2013). Snow redistribution by both wind and avalanches is important on mountain glaciers due to high wind speeds and steep topography. Redistribution of snow significantly alters the mass balance and, thus, melting processes (Wayand et al., 2018). The blowing snow module (Pomeroy, 1989; Pomeroy and Li, 2000) calculates HRU snow erosion and deposition as a mass balance of horizontal snow transport via saltation and suspension and in-transit sublimation using precipitation, wind speed, air temperature and relative humidity as well as information on the snowpack. Horizontal blowing snow redistribution by wind from one HRU to another is determined by exposed surface roughness and therefore snow depth and surface characteristics. Three factors are needed for a blowing snow event to occur – wind at a speed greater than the threshold condition, an open snow surface with good exposure to wind, and supply of erodible snow. Snow

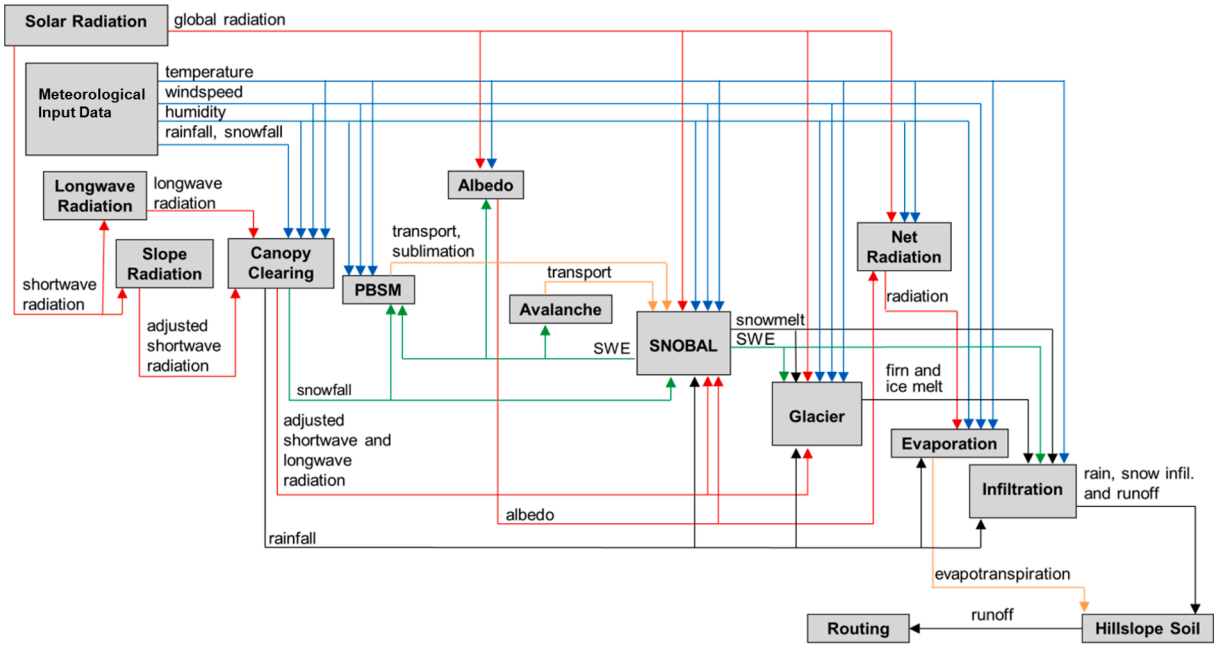

Fig. 3. Modular structure of CRHM-glacier. Red linking arrows are radiation terms; blue lines are climate observations; orange lines are mass transport; green and black lines are model outputs or processed variables of water equivalents, in solid and liquid forms, respectively. (For interpretation of the references to colour in this figure legend, the reader is referred to the web version of this article.)

is eroded from wind-exposed HRUs and deposited as drifts in topographically sheltered or well vegetated HRUs. The details of the blowing snow model in CRHM are provided in Pomeroy et al. (1993) and application of the model over a mountain region is detailed in MacDonald et al. (2009).

In addition to blowing snow, snow is redistributed by gravity in avalanches from higher to lower elevations on steep slopes, described by an avalanche module named as 'SWESlope' (in CRHM) based on the algorithm developed by Bernhardt and Schulz (2010). Snow slides in an avalanche if the minimum snow holding depth (H_d) and a minimum slope angle (S_m) are exceeded. They suggested values of H_d and S_m are 50 mm w.e. (water equivalent) and 25° surface slope, respectively. For slopes steeper than S_m, the snow holding depth decreases exponentially. A best fit regression line (Equation (1)) was derived from the curve of H_d [m] and S_m [^{0}] as developed by Bernhardt and Schulz (2010), and used in the avalanche module.

$$H_d = 3178.4\ S_m^{-2} \tag{1}$$

3.2. Energy balance

The energy available for snow, firn and ice melt (Q_M [W m^{-2}]) is the sum of fluxes due to radiation, turbulence, advection, and conduction (Pomeroy et al., 1998a; Pomeroy et al., 1998b):

$$Q_M = Q_n + Q_h + Q_e + Q_p + Q_g - \frac{dU}{dt} \tag{2}$$

where dU/dt is the change in internal energy of the snow/ice; Q_M is the energy available for melt, Q_p is the advection energy from precipitation, Q_g is the heat flux due to conduction, Q_e and Q_h are turbulent fluxes of latent heat and sensible heat, respectively and Q_n is the net radiation expressed as:

$$Q_n = (K_{in} - K_{out}) + (L_{in} - L_{out}) = (1-\alpha)K_{in} + L_{in} - \varepsilon\sigma T_s^4 \tag{3}$$

where, K_{in} and K_{out} are incoming and outgoing shortwave radiations; L_{in} and L_{out} are incoming and outgoing longwave radiations. All these energy components have units of W m^{-2}. T_s is the surface temperature in Kelvin and ε is the emissivity of the surface. The available energy for melt, Q_M, can be converted to a melt rate, M [m s^{-1}] as:

$$M = \frac{Q_M}{\rho_w L_f} \tag{4}$$

where, ρ_w is the density of water and L_f is the latent heat of water fusion at the freezing temperature. Energy balance glacier melt modelling in CRHM-glacier consists of two separate melt algorithms, giving distinct calculations for snow and firn/ice surfaces. The energy and mass balance snowmelt model - Snobal (Marks et al., 1999; Marks et al., 1998), is used in modelling snow melt processes. It simulates the energy and mass balances of snowpacks in mountains over glacier and non– glacier surfaces. Internal energy exchange is calculated by tracking the cold content in two layers: a) surface-shallow active layer, and b) lower deep snowpack. The model solves for temperature and specific mass [kg m^{-2}], which is the product of snow depth and snow density. Accumulated energy is the energy available after satisfying the cold content and runoff of accumulated melt and liquid content exceeding a specified threshold. The turbulent heat fluxes are obtained using an approach adopted from Brutsaert (1982) by Marks and Dozier (1992). Details are in Marks et al. (1998). A single layer, daily time step, energy budget melt model, originally developed by Gray and Landine (1988) for shallow prairie snowpacks, was customized to ice and firn melt by adjusting its albedo routine and assuming glacier ice and firn are isothermal, so all internal energy change goes to ice melt or firn melt.

The radiation module in CRHM simulates incoming shortwave (global) radiation adjusted to slope and aspect. Similarly, in the absence of observations, longwave irradiance can be estimated from shortwave transmittance and air temperature using the algorithm proposed by Sicart et al. (2006) that modified Brutsaert's clear sky longwave algorithm for cloudy conditions. Terrain emission of longwave is also included in the Sicart's model. The influence of longwave irradiance from surrounding terrain can be significant in mountains (Plüss and Ohmura, 1997). The albedo module of snow evolution by Verseghy (1991) adopted by Essery and Etchevers (2004) based on the age, depth, density and temperature of the snow layer is used to simulate the snow surface albedo.

3.3. Mass balance

CRHM-glacier simulates the mass balance of snow/firn/ice water equivalents for glaciers, as the following variables: snow water equivalent (SWE [mm]), firn water equivalent (FWE [mm]), and ice water equivalent (IWE [mm]). The mass balance of a glacier (MB [mm]), also referred to as the mass budget, is expressed in flux terms as:

$$\frac{dMB}{dt} = \frac{dSWE}{dt} + \frac{dFWE}{dt} + \frac{dIWE}{dt} \tag{5}$$

where, the three terms in the right-hand side are expressed as:

$$\frac{dSWE}{dt} = \frac{dP_{snow}}{dt} + \frac{dH_{in(snow)}}{dt} - \frac{dH_{out(snow)}}{dt} - \frac{dS_{snow}}{dt} - \frac{dM_{snow}}{dt}, \tag{6}$$

$$\frac{dFWE}{dt} = \frac{dV_{in(snow\ to\ firn)}}{dt} - \frac{dV_{out(firn\ to\ ice)}}{dt} - \frac{dS_{firn}}{dt} - \frac{dM_{firn}}{dt}, \tag{7}$$

and

$$\frac{dIWE}{dt} = \frac{dV_{in(firn\ to\ ice)}}{dt} - \frac{dS_{ice}}{dt} - \frac{dM_{ice}}{dt}. \tag{8}$$

SWE, FWE, and IWE are the water equivalents of snow, firn and ice, respectively. Mass balances are typically calculated annually, but fluxes of SWE, FWE and IWE need higher spatial and temporal resolution in their determination. P_{snow} is the amount of precipitation to the snowpack. $H_{in\ (snow)}$ and $H_{out\ (snow)}$ are horizontal incoming and outgoing mass flows of snow due to blowing snow and avalanches, whereas $V_{in\ (snow\ to\ firn)}$ and $V_{out\ (firn\ to\ ice)}$ are vertical incoming and outgoing mass flows due to firnification and firn conversion to ice. S_{snow}, S_{firn}, S_{ice} are the mass losses by sublimation, and M_{snow}, M_{firn}, and M_{ice} are losses by melting from snow, firn, and ice respectively. The units for these variables are mm. P, H_{in}, V_{in} represent input fluxes and H_{out}, V_{out}, S, M represent outputs.

Many models do not consider firn separately (e.g., Li et al., 2015; Naz et al., 2014), however firn has properties that are significant to glacier energetics and mass balance. The albedo of firn is lower than that of snow, but it is higher than that of ice. Secondly, it is important for meltwater routing, which is slower in firn than in ice (Hannah and Gurnell, 2001). Thirdly, the model adds the water equivalents of snow, firn and ice to simulate changes in glacier surface elevation. Glacier surface elevation change (ΔE) at each time step of the model (typically daily) can be obtained as:

$$\Delta E = \frac{\Delta SWE \times \rho_s + \Delta FWE \times \rho_f + \Delta IWE \times \rho_i}{\rho_w} \tag{9}$$

Here, ρ_s, ρ_f, ρ_i, and ρ_w are densities of snow, firn, ice, and water, respectively. The densities are modelled through densification of multilayer snow (Pomeroy et al., 1998a; Pomeroy et al., 1998b) and firn (Herron and Langway, 1980). ΔSWE, ΔFWE, and ΔIWE are changes in water equivalents of snow, firn and ice, respectively.

CRHM simulates the change in glacier surface elevation by considering snow redistribution and accumulation, snow conversion to firn, firn conversion to ice, and ablation of snow, firn and ice. Firn is snow that has survived at least for one summer melt season (Anderson and Benson, 1963). Firn densification is calculated in three temporal stages adopted from semi-empirical steady-state approaches; initially the top

layer snowpack undergoes densification due to wind redistribution and compression as described by Pomeroy et al. (1998a), Pomeroy et al. (1998b). Then firn undergoes densification at a rate that is linearly related to the pressure of overlying snow and firn layers. Herron and Langway (1980) proposed two stages of densification from surface to the zone of pore close-off (~830 kg m^{-3}). The initial rate of densification is faster and occurs until the density reaches 550 kg m^{-3}, considered the critical density, and the latter rate is slower, and proceeds from the critical density to 830 kg m^{-3} from which the firn is considered to have become ice. These firn densification stages are modeled in a 10-layer firn system and one ice layer updated annually at the end of summer. Fig. 4 shows the schematic representation of snow, firn and ice layers transitioning from winter to summer.

3.4. Water flow modules

CRHM assembles hydrological models from a library of physically based hydrological and energy balance process modules. The CRHM-Glacier model considers delayed interflow through snow, firn, ice and subsurface, as well as groundwater flow, using lag and storage hydrograph translation parameters. The concept of linear storage routing has been used in several glacio-hydrological studies (e.g., Engelhardt et al., 2014; Hannah and Gurnell, 2001; Huss *et al.*, 2008; Magnusson et al., 2011; Oerter et al., 1981, Jansson et al., 2003). de Woul et al. (2006) proposed variable snow and ice reservoirs whilst keeping the firn reservoir constant. They considered snow-covered firn to be part of the firn reservoir, however if ice was covered by snow, they considered a distinctive snow reservoir in their model. In CRHM-glacier, meltwater is therefore routed from one HRU to the other until it reaches the outlet by means of three storage constants - ice, firn, and snow. Once the meltwater and rain reach the ground surface, the three modules (infiltration, hillslope, and routing) estimate their storage and flow through three different strata – surface, subsurface and groundwater. The model considers delayed interflow through snow, firn, ice, and subsurface and groundwater flows, using lag and storage parameters, which can be determined using values from the literature or estimated using flow timing measurements or by calibration to fit the streamflow hydrograph.

Either the Muskingum streamflow routing module (Chow, 1959) or Clark's lag and route runoff routing module (Clark, 1945) can be chosen in CRHM for routing runoff to streamflow. Infiltrated water is calculated by a hillslope soil module by Fang et al. (2013), based on the soil module by Leavesley et al. (1983), which was progressively modified by Dornes et al. (2008) for cold regions mountain soils and Fang et al. (2010) for depressional storage and Fang et al. (2013) for mountain hillslopes. The hillslope soil module deals with depression storage, subsurface runoff, groundwater recharge, and groundwater flows between HRUs. Water moisture loss from unsaturated or saturated non-frozen surfaces by evaporation and transpiration is estimated using Granger-Gray's evapotranspiration expression (Granger and Gray, 1989; Granger and Pomeroy, 1997), which employs an energy budget and an extension of Penman's combination equation using the complementary evaporation hypothesis. Evaporation from open water bodies is simulated by the energy budget evaporation expression for small water bodies and wetlands developed by Priestley and Taylor (1972).

3.5. Hydrological response units (HRUs)

The basins were discretized into HRU based on slope, aspect, elevation and landcover (including glacier cover). The HRU are control volumes used to apply meteorological forcing data and are the basis for coupled mass and energy budgets by the process modules. Google Earth Engine and ArcMap were used to prepare HRUs for both basins. The steps in the flowchart shown in Fig. 5 (example for PGRB) were followed for the two research basins, PGRB (Fig. 6) and AGRB (Fig. 7). Two landcovers, 2014 and 1966 in the case of PGRB and 1984 and 2014 in the case of AGRB were used. Since the gauging sites were at different locations during the IHD period and the present time, two separate basin maps were prepared for PGRB. The catchment area at the new gauging site is about 4 km^2 smaller than at the old gauging site.

Except for the 1966 landcover map of PGRB, Landsat images taken between 15th July to 15th September were considered as this time of year when the seasonal snowpack has melted. The PGRB landcover map for 1966 was prepared from the scanned topographic map of 1966. Four landcover classes were considered: accumulation area (firn/snow), ablation area (ice), non-glacierized area (bare), and water. The following steps were considered whilst preparing HRU.

1. Landcover maps from two periods were prepared from Landsat images and a topographic map. For AGRB, 1984 and 2014 and for PGRB 1966 and 2014 were considered.
2. DEM derivatives slope, aspect and elevation bands were created from 2000 DEM (AGRB) and 1966 DEM (PGRB) using the ArcMap spatial analyst tool.
3. Slope was reclassified to 3 classes (0-15°, 15-45°, and > 45°); aspect was reclassified to North and South; and elevation was classified in bands at every 100 m. The classes were converted to polygons using a raster to polygon tool.
4. Landcovers from two dates, slope, aspect and elevation bands were intersected with each other using the union function.
5. The created feature had many smaller polygons, which were simplified using the Eliminate function. The smaller polygons with area below 25000 m^2 were dissolved to polygon with the largest border it shared with.
6. If the polygons fell under bare area on both years (1984 and 2014 for AGRB and 1966 and 2014 for PGRB), the polygons were merged to adjacent polygons making elevation bands cut at every 200 m.

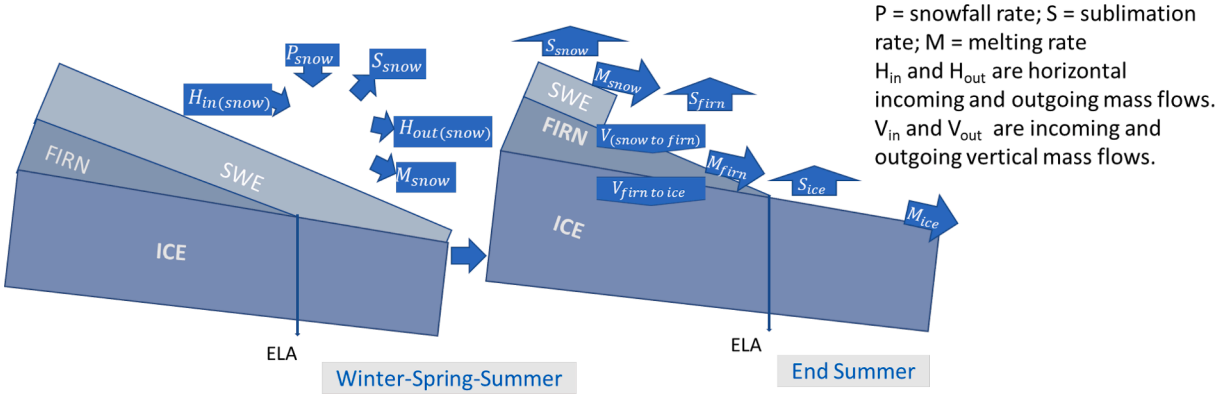

Fig. 4. CRHM-glacier simulates the mass balance of snow water equivalent (SWE [mm]), firn water equivalent (FWE [mm]), and ice water equivalent (IWE [mm]) and interactions amongst these frozen reservoirs.

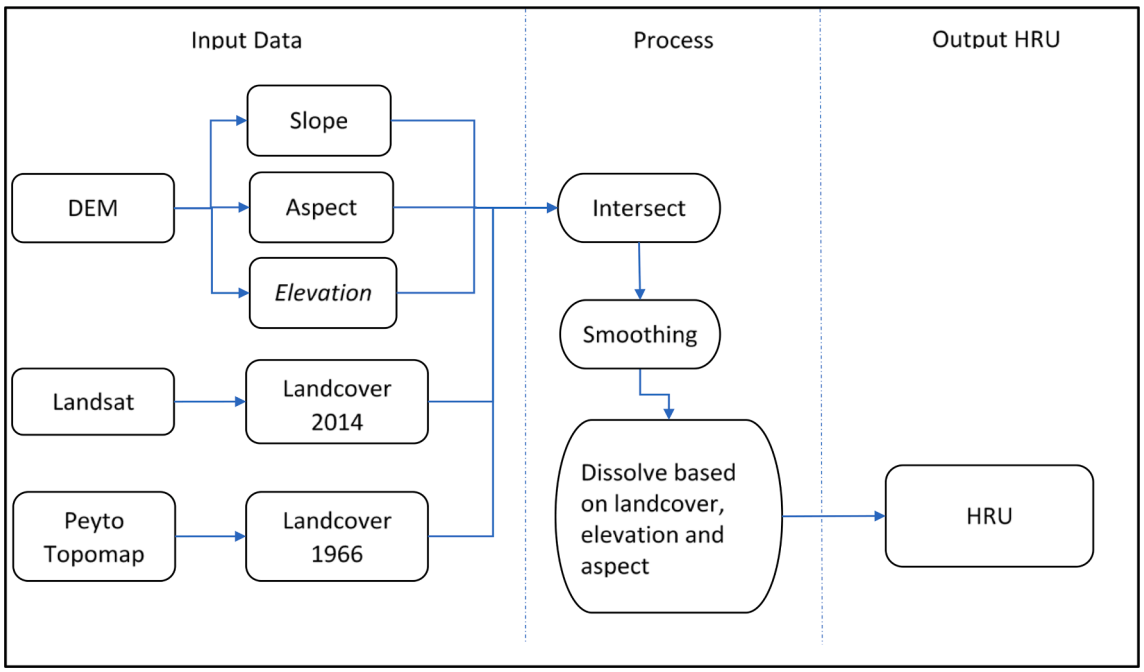

Fig. 5. Flowchart showing the process for delineating HRUs.

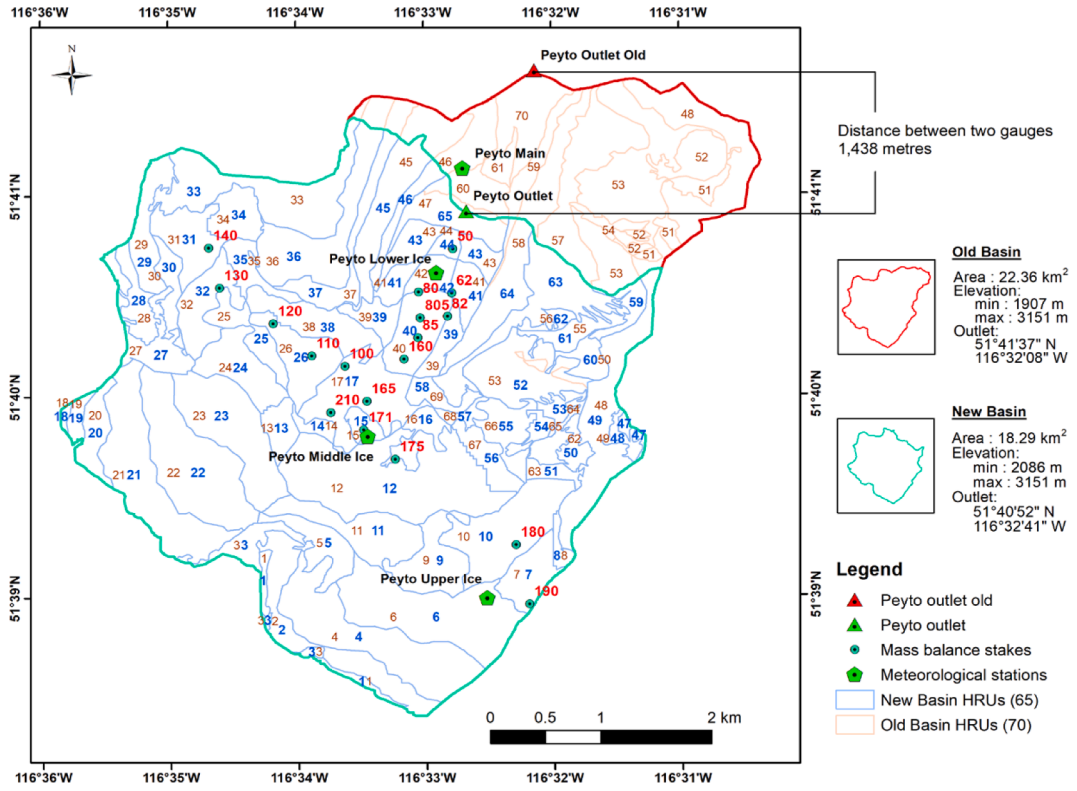

Fig. 6. PGRB with two outlets, Peyto Outlet Old and Peyto Outlet. The old basin has 70 HRUs [light red numbers] and the new basin 65 HRUs [blue numbers]. Bold red numbers are mass balance stakes. (For interpretation of the references to colour in this figure legend, the reader is referred to the web version of this article.)

7. All the polygons were carefully analyzed based on topology and merged to one another reducing the number of HRU's to 90 for AGRB (Fig. 6) and 70 for PGRB (Peyto Old Outlet). The number of HRU's were reduced to 65 for PGRB with Peyto New Outlet (Fig. 7).
8. HRU numbering was done based on flow direction patterns where water flows from smaller HRU number to higher HRU number, finally towards the outlets of the basins. HRU 90 is the outlet of AGRB, HRU 70 is the Peyto Old Outlet and HRU 65 is the Peyto New Outlet.

The physiographic parameters required by CRHM-glacier for each HRU include the following: area, latitude, average elevation, average

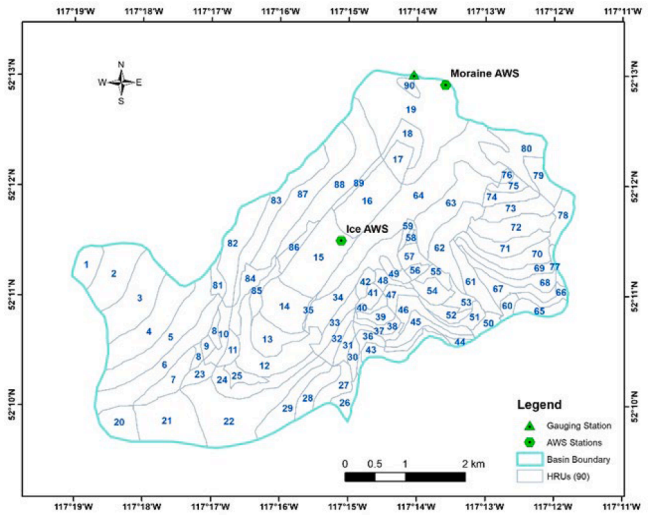

Fig. 7. AGRB with 90 HRUs, two AWS, and the outlet station. Blue numbers are HRUs. (For interpretation of the references to colour in this figure legend, the reader is referred to the web version of this article.)

ground slope, average aspect and average terrain view factor (TVF). Except for TVF, all parameters were calculated in R for each available DEM. TVF was obtained in SAGA GIS as a sub-product of the sky view factor under the terrain analysis. The major landcover of each HRU in a year was calculated using 'Zonal Statistics with Table'. The majority of landcovers from 1966, and 2014, in the case of PGRB, and those from 1984 and 2014, in the case of AGRB were calculated by using the raster iterator operator in a model builder of ArcGIS 10.3.1.

3.6. Testing model performance

Model simulations were compared with the available hydrometeorological and glaciological observations at the two basins, AGRB and PGRB to evaluate the CRHM-glacier model. The model was compared with the *in-situ* measurements of albedo, surface accumulation and ablation, and streamflow discharge generation. Incoming and outgoing shortwave radiation measured by AWS on glacier ice and moraine provided observed albedo. Measured daily albedo was obtained as a ratio of the daily amount of outgoing shortwave radiation to the daily amount of incoming shortwave radiation (Oerlemans and Knap, 1998). Daily observed and simulated albedo values were compared for the four sites for five years or more except Peyto Glacier Lower Ice AWS, which had both incoming and outgoing shortwave radiation measurements during 2007–2008 only.

Modelled surface accumulation and ablation processes over the glacier were compared with surface height changes (Fig. 8) that were measured by SR50 ultrasonic depth sounders at the three ice stations in PGRB. The advantage of comparing surface elevation change over comparing water equivalent change is that the former provides an additional comparison of density simulation in the model (Garen and Marks, 2005). This process also validates the surface elevation change modelled by the accumulation and ablation process at the surface.

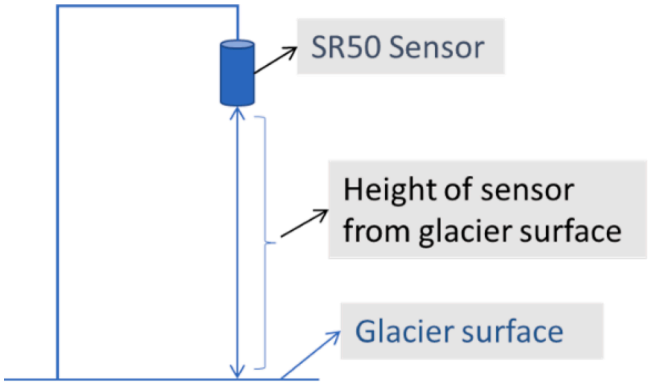

Fig. 8. Schematic diagram of the SR50 ultrasonic depth sensor above the glacier surface measuring change in glacier surface elevation.

CRHM parameters were set by knowledge and understanding of the basin, instead of optimizing to simulate the streamflow hydrograph. Though parameter calibration is sometimes inevitable, it can be reduced with advancements in hydrological science (Pomeroy et al., 2013). Ommanney (2002) summarized the studies made by Derikx (1975) and Collins (1982) who found that the meltwater reaches the outlet of PGRB at a very short time, from 2 to 5 h. Munro (2011a) and Munro (2013) also considered the runoff delay in PGRB, and found it varied from a few hours to half a day. Given the daily time step of discharge, no parameters whatsoever were calibrated in this study. The model simulated discharges of the two basins for two different time slices were compared with observations over daily periods for the present (2014–2019 for AGRB; 2013–2018 for PGRB) and past datasets (1967–1977 and 1980–1989 for AGRB; 1967–1977 for PGRB).

CRHM-glacier considered redistribution of accumulated snow by two processes, blowing snow and avalanching. Blowing snow includes the effect of blowing snow transport, redistribution and sublimation losses. Avalanching is dependent upon blowing snow transport to redistribute snow to form deep accumulations in avalanche source areas. The effects on model performance of adding blowing snow and avalanching were investigated using model falsification, with and without these processes, by comparing the model outputs to the observations. Similarly, the test runs were carried out to diagnose the impacts of glacier processes on the model. Model falsification is straightforward to implement in CRHM. The blowing snow, avalanche and glacier modules in CRHM can be turned on and off so that outputs could be compared. For example, models could be built with and without the blowing snow module. First, the model was tested for glacier surface elevation changes on Peyto Glacier at three observational sites. Second, it was tested for streamflow simulations from the two basins, AGRB (for 2014–2019) and PGRB (2013–2018) with forcing meteorological data from bias-corrected ERA-Interim and *in-situ* observed data. The following three model scenarios were considered with a model falsification approach to examine the impacts of glacier and snow redistribution processes on streamflow and glacier surface calculations.

1. With both glacier and snow redistribution processes.
2. With glacier, but without snow redistribution processes.
3. With snow redistribution, but without glacier processes.

Based on these three experimental scenarios, three comparison tests were employed to evaluate the glacier and snow redistribution modules.

Agreement between simulated and observed values was evaluated by using both traditional and non-traditional statistical indices. Nash-Sutcliffe efficiency (NSE, Nash and Sutcliffe, 1970), mean bias error (MBE) and the root mean square error (RSME) were used, along with the Wang-Bovik Index (WBI), proposed by Wang and Bovik (2002) and reformulated by Mo et al. (2014) for application to hydrometeorological data. WBI evaluates the similarities between modelled and observed variables in terms of pattern association and differences in the means and variances (Mo et al., 2014).

$$WBI = [m_{xy}][v_{xy}][R_{xy}] \tag{10}$$

where, the three components are defined as:

$$m_{xy} = \left[\frac{2(\bar{x} - \psi_{xy})(\bar{y} - \psi_{xy})}{(\bar{x} - \psi_{xy})^2 + (\bar{y} - \psi_{xy})^2}\right] \tag{11}$$

$$v_{xy} = \left[\frac{2\sigma_x\sigma_y}{\sigma_x^2 + \sigma_y^2}\right] \quad (12)$$

$$R_{xy} = \left[\frac{\sigma_{xy}}{\sigma_x\sigma_y}\right] \quad (13)$$

where, ψ_{xy} = min (x_i, y_i | i = 1,2, 3, ...N). Here x_i and y_i are measured and predicted daily global solar radiation, respectively, at i day. $\bar{x}$ and $\bar{y}$ are means, σ_x and σ_y are standard deviations, and σ_{xy} is covariance. m_{xy} and v_{xy} are the measures of differences in means and variances, respectively. R_{xy} is the Pearson correlation coefficient. All statistical analyses were carried out in R (R Core Team, 2017) in the RStudio platform (RStudio, 2017). The code for WBI was provided by Paul Whitfield (University of Saskatchewan Centre for Hydrology and Environment and Climate Change Canada); and the other codes were used from the R packages hydroGOF (Mauricio, 2014) and sirad (Bojanowski, 2016). The analysis results are presented in graphs and tables. Performance rating based on the values of NSE was considered as 'very good' [NSE > 0.65], 'adequate' [0.65 => NSE > 0.54], and 'satisfactory' [0.54 => NSE > 0.50] following Dahal et al. (2020).

4. Results and discussion

Unlike other glacier hydrological models, the model parameters in CRHM-glacier are not calibrated, and so there are no calibration and validation periods to compare. The model results are presented in the following subsections.

4.1. Model evaluation

The model was tested against observations of meteorological variables, albedo, mass balance and discharge. Model performance was evaluated by means of visual as well as statistical interpretations.

4.1.1. Albedo

Net shortwave radiation is the most important energy flux for glacier melt (Munro and Young, 1982). Therefore, accurate parameterization and modelling of surface albedo are crucial for computing the energy and mass balance of the glaciers. The model was evaluated using recent measurements of surface albedo at four locations - two sites in PGRB (Peyto Main and Peyto Lower Ice stations) and two sites in AGRB (Athabasca Moraine and Athabasca Ice stations). The CRHM-glacier albedo module was used to simulate albedo on glacier ice and off glacier surfaces over both basins. The meteorological forcing data for these tests were from Athabasca Moraine station for AGRB and Peyto Main station (except precipitation data) for PGRB. Precipitation data for PGRB were from Bow Summit. The comparisons were made at daily values with point AWS measurements (Fig. 9) and their statistical measures for model performance are presented in Table 4.

The model captured the variation of albedo on both on-ice and off-ice sites with WBI higher than 0.85, RMSE less than 0.17 and the highest MBE being 0.063. Though these point observations do not represent all basin areas, they represent both snow accumulation and ablation

Table 4
Comparison of *in-situ* observed, and CRHM-glacier simulated albedo.

Research site	Surface type	Elevation (m)	Data period (number of days)	MBE	RMSE	WBI
AGRB	Ice	2177	2014–2019 (1475)	−0.047	0.142	0.86
	Moraine	1974	2014–2019 (1760)	0.063	0.170	0.85
PGRB	Ice	1973	2007–2008 (731)	0.007	0.117	0.88
	Moraine	2250	2013–2019 (2266)	0.030	0.129	0.91

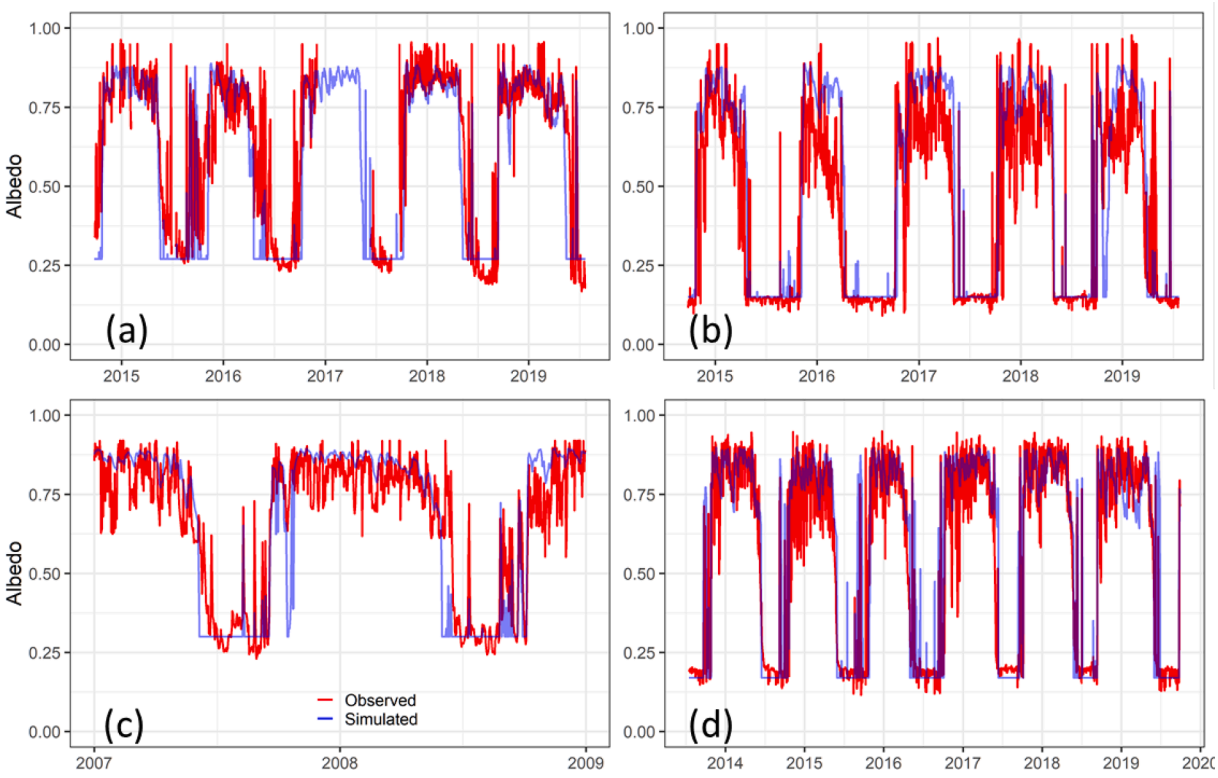

Fig. 9. Albedo simulations, measured (red lines) and simulated (blue lines). (a) Athabasca Ice station (2014–2019); (b) Athabasca Moraine station (2014–2019); (c) Peyto Lower Ice station (2007–2008); (d) Peyto Main station (2013–2019). (For interpretation of the references to colour in this figure legend, the reader is referred to the web version of this article.)

conditions. Since a single value of albedo was used for snow-free conditions, the variation of albedo during ice melt was not represented. However, transitions of albedo from snow-covered to snow-free and vice versa were well captured at both on-ice and off-ice sites (Fig. 9). Both glacier and moraine sites presented cycles of snow-covered and snow-free times, with albedo values reaching 0.9 and 0.3 in the case of ice surfaces, and 0.15 at moraines. The ice-exposed periods with lower albedo values were well simulated by the model. The modelled albedo decay over the Athabasca Moraine station was slower than the observed values and mid-winter albedo values were overestimated due to wind erosion of snow and exposed boulders and microtopography at this site. The albedo of Athabasca Ice during snow free periods in the recent years (2017–2019) was lower (<0.25) than the previous years (Fig. 9a) and may be influenced by upwind forest fires (Bertoncini et al., in review).

4.1.2. Glacier mass balance

The surface accumulation and ablation simulations from CRHM-glacier were tested with the surface mass balance measurements by mass balance stakes and ultrasonic sensors (SR50) installed at various points over Peyto Glacier.

4.1.2.1. Surface point mass balance. Fig. 10 shows the time series of simulated and observed changes in the elevation of the glacier surface with respect to the SR50 sensors during the recent decade. The model was run from October 2010 to September 2019 with meteorological forcing data from both *in-situ* observation at Peyto Main station (air temperature, relative humidity, wind speed, incoming short- and long-wave radiation) and Bow Summit (precipitation) and bias-corrected ERA-Interim. The comparisons were limited to the periods when SR50 data were available. Performance of the model along with

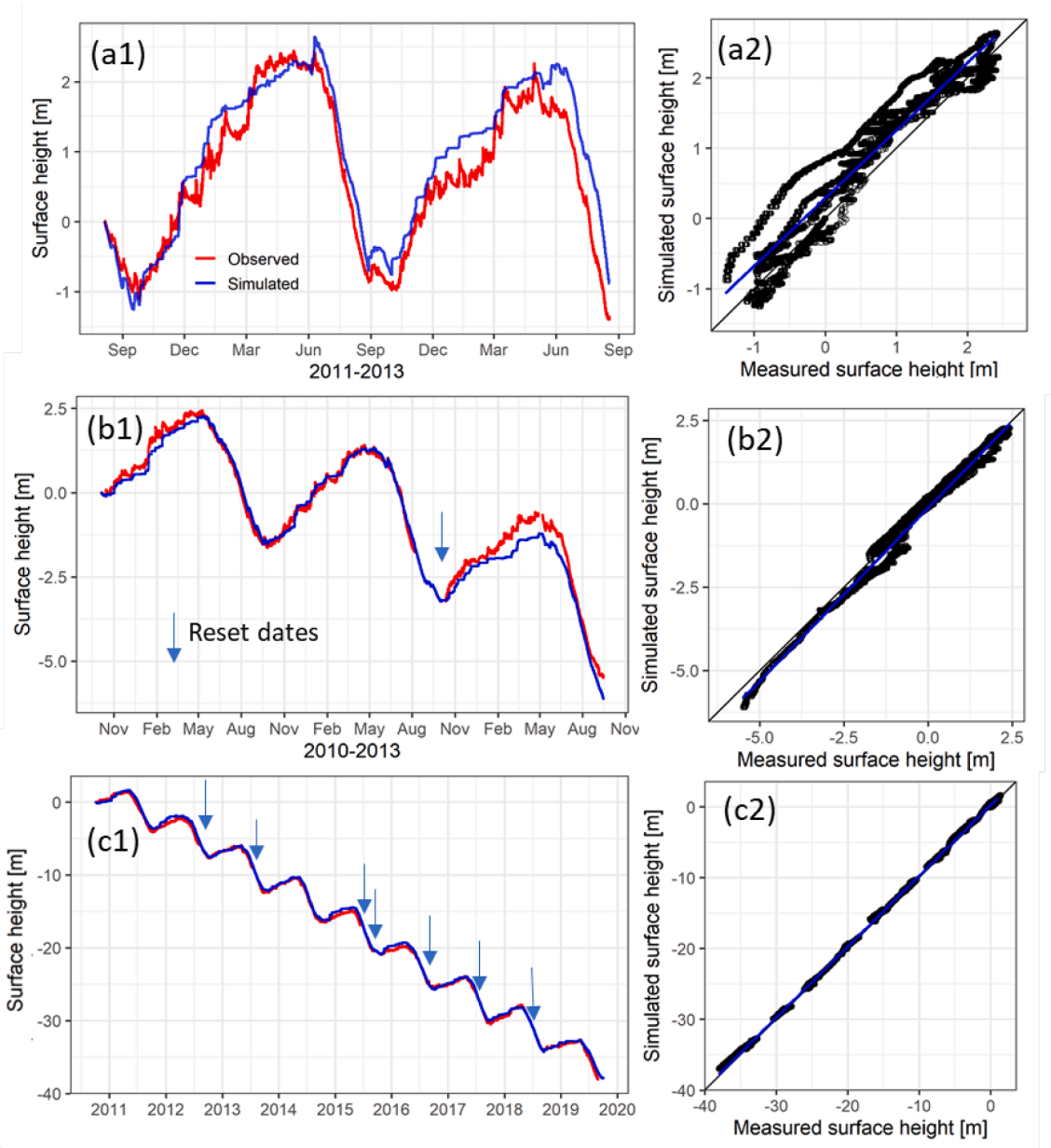

Fig. 10. Simulated surface accumulation and ablation averaged to daily values as represented by the change in glacier surface elevation with respect to the height of sonic ranger sensor at the ice stations of Peyto Glacier. (a) Upper Ice station, (b) Middle Ice station, and (c) Lower Ice station. a2, b2, and c2 are scatter plots between measured and simulated surface heights. Black is 1:1 line, and blue is the best fit line by applying a linear regression. Resets are the adjustments of the SR50 to new heights, and they are brought to coincide with the simulated values of the same dates. Blue is model simulated height and red is the measured height from SR50. (For interpretation of the references to colour in this figure legend, the reader is referred to the web version of this article.)

meteorological forcing data were evaluated by statistical parameters presented in Table 5.

All the sites had at least one continuous dataset for two years showing the model's capability to capture accumulation and ablation. The best match between simulated and observed surface heights was at the lower ice station and performance diminished with elevation. The model accumulated more mass during the two-year period than the measured mass balance at the Upper Ice station (MBE = 0.26 m) with the measured model forcing data from the Peyto Main. However, the accumulation was less when the model was forced with ERA-Interim data (Table 5).

4.1.2.2. Aggregated glacier mass balance. Model-simulated hourly/daily mass balance for Peyto Glacier was converted to seasonal and annual mass balances to compare with the measured values obtained from the ablation stakes (Fig. 6). The simulated seasonal glacier mass balances exclude Dragan Glacier and other small ice patches in the northeast part of the basin for the period from 1965 to 1995. Fig. 11 shows that the model did not simulate the aggregated seasonal mass balance as well as it simulated point mass balances, as presented in section 4.1.2.1. Several factors could have contributed to the reduced performance at the glacier scale. Firstly, none of the model parameters were calibrated to simulate mass balance, although there is a practice of calibrating mass balance against *in-situ* observations (e.g., Giesen and Oerlemans, 2012; Radić and Hock, 2011; Shannon et al., 2019). Secondly, the model performed less well at the Upper Ice station compared to the Middle Ice and Lower Ice stations (Fig. 10). Another reason could be the difference in approaches to obtain the seasonal mass balance. The observed values of seasonal mass balance were obtained from a series of transects of ablation stakes, distributed over half of the glacier area at lower elevations (Fig. 6), and these values were linearly extrapolated to higher elevation bands, as there were not any mass balance stake measurements above 2700 m (details are in Demuth and Keller, 2006). The modelled seasonal mass balance was calculated from the HRUs distributed over the glacier. Differences between the mass balance extrapolations and various model distributions of forcing meteorology with elevation could explain why the mass balances simulated at lower elevation bands matched closer to the observations (not shown here) than did those simulated at higher elevation bands.

4.1.3. Streamflow

Model performance metrics for both basins are provided in Table 6 and from Figs. 12 to 15. The performance of the model can be rated as 'very good' with NSE equal to 0.71 and 0.77 for AGRB for the period 2014–2019 with meteorological forcing data from *in-situ* observation and from ERA-Interim, respectively. The model performance of AGRB with ERA-40 forcing data was also 'very good' for the past records, 1967–1977 (NSE = 0.75) and 1980–1989 (NSE = 0.73). The model performance for PGRB was 'very good' with NSE equal to 0.68 and 0.67 with meteorological forcing data from in-situ observation and from ERA-Interim, respectively. WBI values were 0.86 and 0.87 for AGRB and 0.80 for PGRB. However, PGRB had smaller MBE values (-0.06 and −0.01 m^3s^{-1}) and lower RMSE values (1.19 and 1.2 m^3s^{-1}) than AGRB (MBE, 0.28 and −0.11 m^3s^{-1}; RMSE, 1.29 and 1.14 m^3s^{-1}) (Figs. 13-15).

The model also performed well for the past records with bias-corrected ERA-40. NSE values of AGRB were 0.75 and 0.73 and WBI were 0.89 and 0.87 for the periods 1967–1977 and 1980–1989 respectively. The NSE value of PGRB (1967–1977) was 0.61 with the bias corrected ERA-40. The model was also tested with Lake Louise precipitation data for PGRB (1967–1977). The model driven by ERA-40 data provided a better simulation than that driven by ERA-40 with Lake Louise precipitation data (Table 6).

Generally, the model simulated streamflow well, with WBI values higher than 0.8 except for PGRB in the past (1967–1977) when the WBI was 0.76. WBI evaluates similarity in modelled and simulated values in terms of not only correlation, but also mean and variance (Mo et al., 2014). The model performed better in AGRB compared to PGRB. Moreover, the streamflow simulations were better in the present period compared to the past for PGRB. This could be due to the uncertain quality of streamflow data at PGRB in the past. Flow measurement at the Peyto outlet during the IHD (1967–1977) was a challenge due to an unstable cross section, occasional flash floods, and lack of direct discharge measurements during high flows. Goodison (1972) reported that the discharge records from 1967 were not reliable and he did not use this data for his study. The streamflow stage gauge was washed out during a flood in August 1967. Occasional flash floods were reported in the stream by Ommanney (1987) and Johnson and Power (1985). However, model performance statistics show a good ability to simulate streamflow both in the past and present time periods from the bias-corrected reanalysis data for both basins.

The test runs were also carried out to see the impacts of glacier and snow redistribution processes using a model falsification approach (Fang et al., 2013). The model was run three times, first with both glacier and snow redistribution processes. The second run was with the glacier, but without snow redistribution processes, and the third one was with snow redistribution, but without the glacier. Fig. 16 compares the observed and simulated streamflow hydrographs for AGRB, averaged over the model run period of 2014–2019. Streamflow simulations without the glacier generated about 50% of the observed flow and indicated the strong influence of glaciation on streamflow. The differences between observed and simulated streamflow without the glacier were highest during July-August. Fig. 17 compares these simulations with the observed streamflow at the Peyto Glacier outlet. Similar to Athabasca, hydrological simulations without the glacier in PGRB also generated almost half the streamflow compared to the observed streamflow. Simulations without snow redistribution overestimated streamflow, showing the need to include blowing snow transport and sublimation calculations in glacier hydrological simulations. The agreement between simulated and observed runoff was closer in PGRB than in AGRB. This is likely due to the precipitation data used. For PGRB this was observed at the Bow Summit station, which is a well-sheltered precipitation gauge, whereas the precipitation gauge in AGRB is at wind-blown open site where uncertainty due to wind undercatch corrections is introduced. Moreover, the precipitation and temperature lapse rates were determined from observed precipitation at different elevations at PGRB and these values were transferred to AGRB, adding uncertainty in the regionalization of these rates.

Table 5
Statistical matrix of mass balance simulation at different sites using *in-situ* and ERA-Interim data.

Site	Data period (number)	Forcing data	Slope	Intercept (m)	WBI	NSE	RMSE (m)	MBE (m)
Peyto Upper Ice station	2011–2013 (17855)	*In-situ*	0.96	0.35	0.96	0.863	0.39	0.26
		ERA-I	1.02	−0.74	0.91	0.424	0.80	−0.69
Peyto Middle Ice station	2010–2013 (23235)	*In-situ*	1.04	−0.13	0.99	0.975	0.27	−0.14
		ERA-I	1	−0.38	0.98	0.943	0.48	−0.38
Peyto Lower Ice station	2010–2019 (63630)	*In-situ*	1	0.23	1	0.998	0.36	0.23
		ERA-I	1	0.25	1	0.998	0.40	0.21

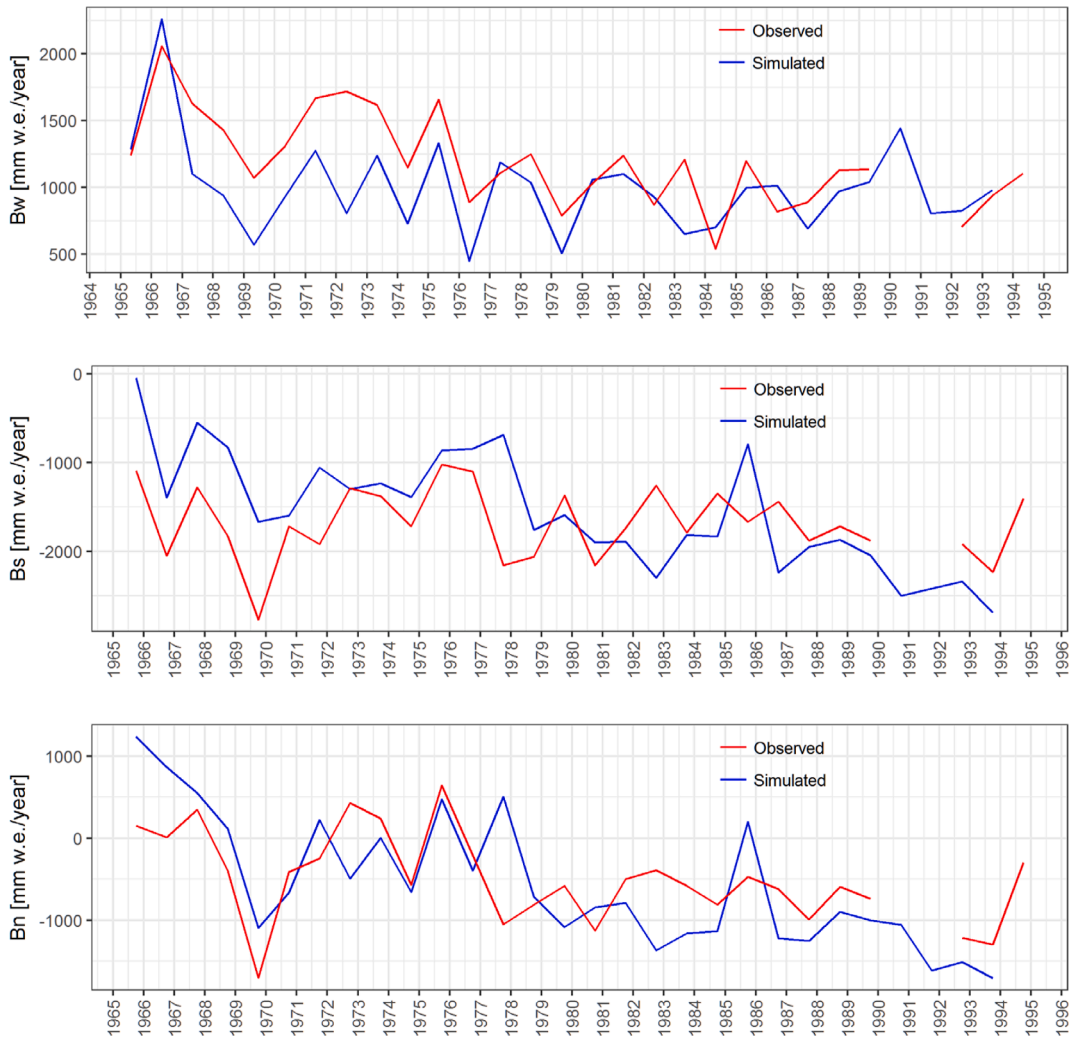

Fig. 11. Mass balance simulation for the Peyto Glacier. Bw: winter balance, Bs: summer balance, Bn: net mass balance. Blue is simulated, and red is observed. (For interpretation of the references to colour in this figure legend, the reader is referred to the web version of this article.)

Table 6
Statistical matrix for the streamflow simulations.

Research basins	Meteorological forcing data	Simulation periods	MBE [m^3s^{-1}]	RMSE [m^3s^{-1}]	WBI	NSE
AGRB	*In-situ*, Athabasca Moraine (t, e_a, u, Q_{si}, Q_{li}, p)	2014–2019	0.28	1.28	0.86	0.71
	ERA-Interim (t, e_a, u, Q_{si}, Q_{li}, p)	2014–2019	0.11	1.14	0.87	0.77
	ERA-40 (t, e_a, u, Q_{si}, Q_{li}, p)	1967–1977	0.19	1.09	0.89	0.75
	ERA-40 (t, e_a, u, Q_{si}, Q_{li}, p)	1980–1989	0.17	1.14	0.87	0.73
PGRB	*In-situ*, Peyto Main (t, e_a, u, Q_{si}, Q_{li}), Bow Summit (p)	2013–2018	−0.06	1.19	0.80	0.68
	ERA-Interim (t, e_a, u, Q_{si}, Q_{li}, p)	2013–2018	−0.01	1.20	0.80	0.67
	ERA-40 (t, e_a, u, Q_{si}, Q_{li}, p)	1967–1977	−0.45	1.74	0.76	0.61
	ERA-40 (t, e_a, u, Q_{si}, Q_{li}) and Lake Louise (ppt)	1967–1977	−0.42	1.87	0.73	0.56

4.2. Sources of runoff and changes over time

The CRHM-glacier model was used to determine various spatially integrated mass fluxes and their changes over a period of five decades. Simulated, spatially integrated mass fluxes are shown in Fig. 18; their values are given in Table 7. This shows the importance of glacier firn and ice melt (38–50%) to total runoff (streamflow discharge), though snow melt was still the largest runoff component. The contribution of glacier melt increased by 6–7% in the recent decade (2006–2017) compared to the past (1966–1977). Total precipitation decreased in both basins however the rainfall ratio increased as did basin flow (annual discharge). This was caused by an increase in glacier ice melt that was tempered by a decrease in snow melt. The combination of increasing rainfall, decreasing snow melt, increasing ice melt led to increasing basin flow and showed a hydrological regime change under way. Importantly, the increase in rainfall and ice melt more than compensated for decreasing snow melt in their impact on basin flow.

5. Discussion

Most mountain glaciers lack on-ice weather data (Clarke et al., 2009). The result of CRHM-glacier over Peyto and Athabasca glaciers is encouraging, in that both off-ice station and atmospheric model reanalysis data have very good potential for use in driving glacier

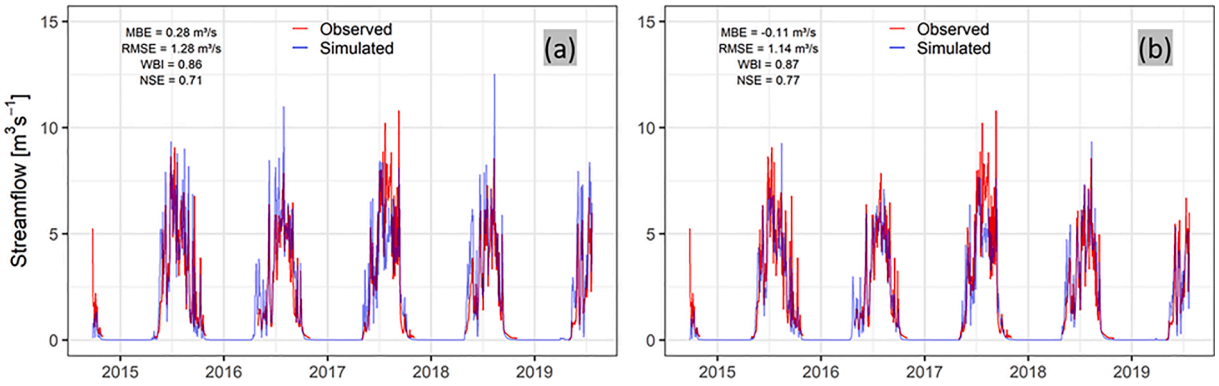

Fig. 12. Daily mean streamflow discharge at Athabasca Glacier outlet [2014–2019], (a) simulated from *in-situ* observed meteorological forcing data (b) simulated from the bias corrected ERA-Interim.

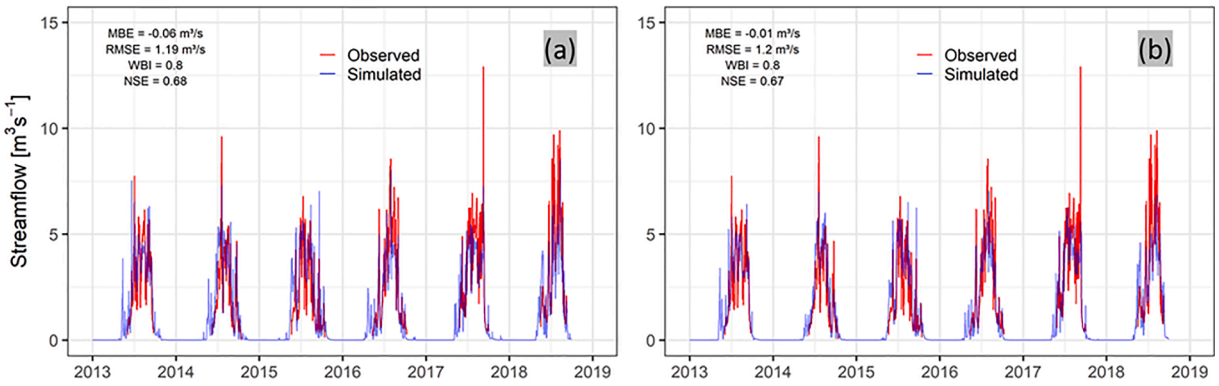

Fig. 13. Daily mean streamflow discharge at the Peyto Glacier outlet [2013–2018], (a) simulated from *in-situ* observed meteorological forcing data measured at Peyto Main (t, rh, u, Q_{si}, Q_{li}) and Bow Summit (ppt) (b) simulated from the bias corrected ERA-Interim meteorological forcing data.

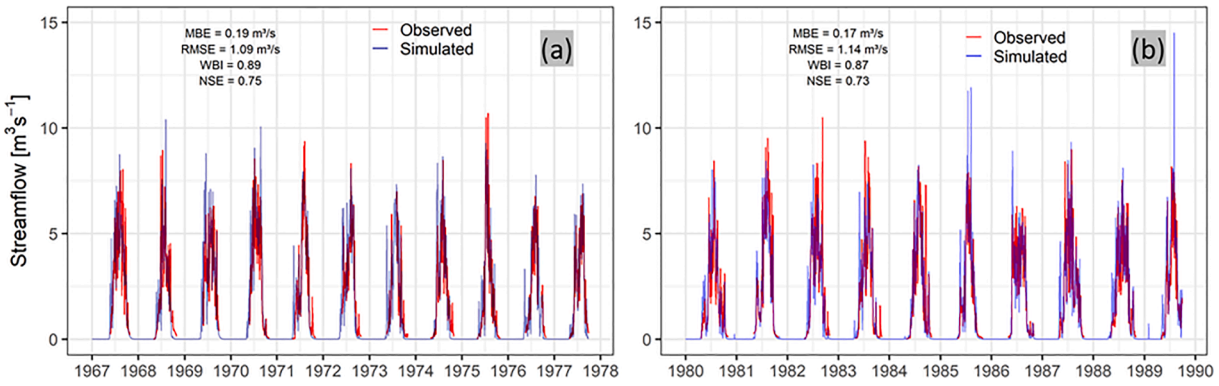

Fig. 14. Daily mean streamflow discharge at the Athabasca Glacier outlet simulated from the bias corrected ERA-40 forcing data; a) [1967–1977] and b) [1980–1989].

hydrological models of mountain glaciers in remote regions.

The simulated streamflow hydrographs without the glacier generated about half of the total observed flow in both basins. The differences in these flow values increased to approximately an order of magnitude larger than modelled flows without the glacier by late summer when ice melt is large and snow melt is depleted. These test runs showed that the streamflow from these basins would be reduced dramatically and catastrophically under the current climate with complete deglaciation. Snow redistribution processes by wind and avalanches reduced streamflow. The simulation with the glacier and addition of the redistribution processes reduced the differences between the simulated and observed streamflows and were important to include.

The shifting importance of glacio-hydrological processes from the IHD period to the present is instructive. The increase in rainfall and decrease in snowmelt can be attributed to the increasing rainfall ratio and its effects on both rainfall occurrence and snow accumulation and melt. The declining snowcover over the glaciers increased the ice exposure and hence the ice melt, as there was a greater ice surface exposed to melt energy. This is consistent with the rise in the ELA that is noticeable from the IHD to present period in photographs of Peyto Glacier and the authors' photographs of Athabasca Glacier from the 1970 s to present. The more negative mass balance and shrinkage of both glaciers is the cause of the 260 mm (Peyto) to 88 mm (Athabasca) increase in streamflow runoff when precipitation has declined by 226

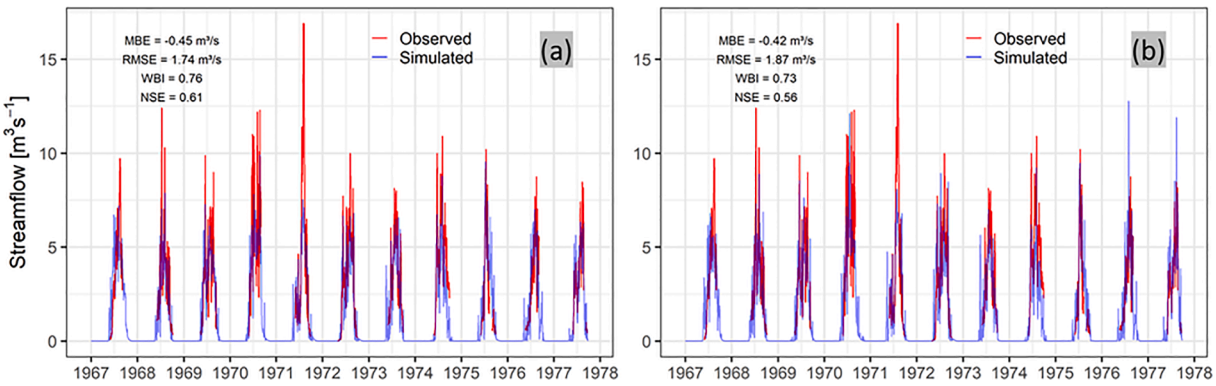

Fig. 15. Daily mean streamflow discharge at the Peyto Glacier outlet [1967–1977], (a) simulated from the bias corrected ERA-40, (b) simulated from the bias corrected ERA-40 (t, rh, u, Q_{si}, Q_{li}) and bias corrected Lake Louise [ppt].

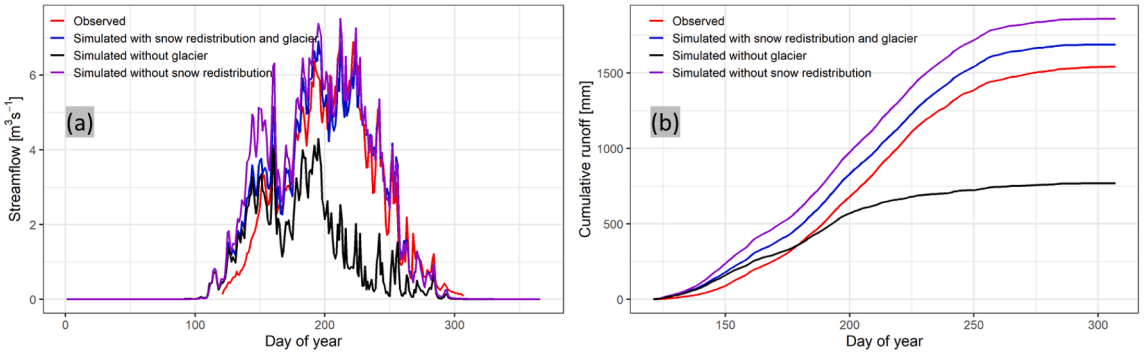

Fig. 16. Simulation of streamflow discharge of AGRB with and without glacier and snow redistribution processes [Meteorological forcing data from Athabasca Moraine station]; (a) daily averaged values for the period, 2014–2019, (b) averaged cumulative runoff values.

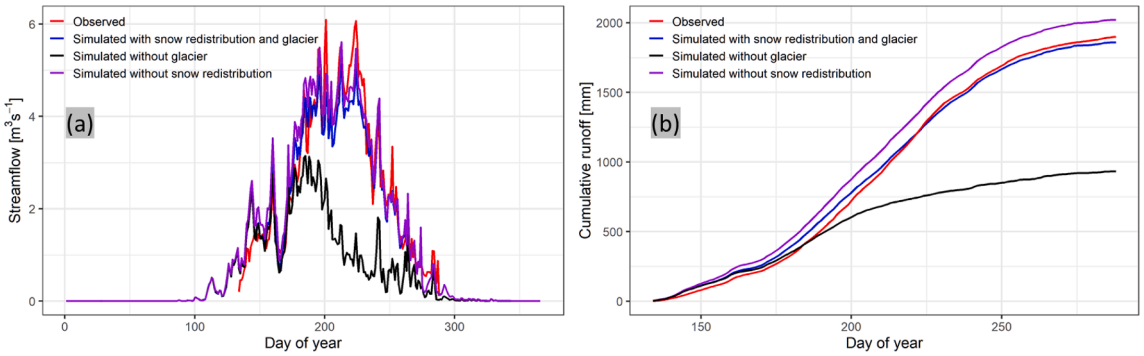

Fig. 17. Simulation of streamflow discharge of PGRB with and without glacier and snow redistribution processes; (a) daily averaged values for the period, 2013–2018, (b) averaged cumulative runoff values.

mm (Peyto) and 115 mm (Athabasca) since the 1960 s.

Though the model performed well in most tested metrics, there are some limitations that could be improved in future studies. CRHM-glacier was constrained by the forcing of meteorology and the suite of processes that were included in the model. Several uncertainties in the input data drove the uncertainties in model outputs. Precipitation is critical for CRHM-glacier. Precipitation measurements at the moraine stations in the study basins were not reliable due to very high wind speeds for which available undercatch equations are unreliable. Therefore, precipitation measured at Bow Summit, a small wind-sheltered forest clearing outside PGRB, was used to evaluate model performance and to bias correct reanalysis data. No similar sheltered precipitation gauge was available for AGRB. The temperature and precipitation lapse rates were set by observations made at different elevations and so errors in these observations propagated into lapse rate estimation.

Another important meteorological variable is shortwave irradiance. The model corrects irradiance due to self-shading for each HRU, using slope and aspect to spatially distribute shortwave and longwave irradiance. However, it does not consider shadowing from surrounding topography, consideration of which may improve melt calculations in mountains as shown by Marsh et al. (2012) and Hopkinson et al. (2010) in this region. Moreover, there are potential errors in global radiation measurement. Average global radiation was measured with a Kipp and Zonen CM-11 pyranometer and a CNR-4 in the main stations. Snow accumulation and frost on the pyranometer dome certainly occurred at times.

Similarly, several processes such as ice flow, glacier surges, melt of ice-cored moraine, ice falls, ice calving into the downstream glacial

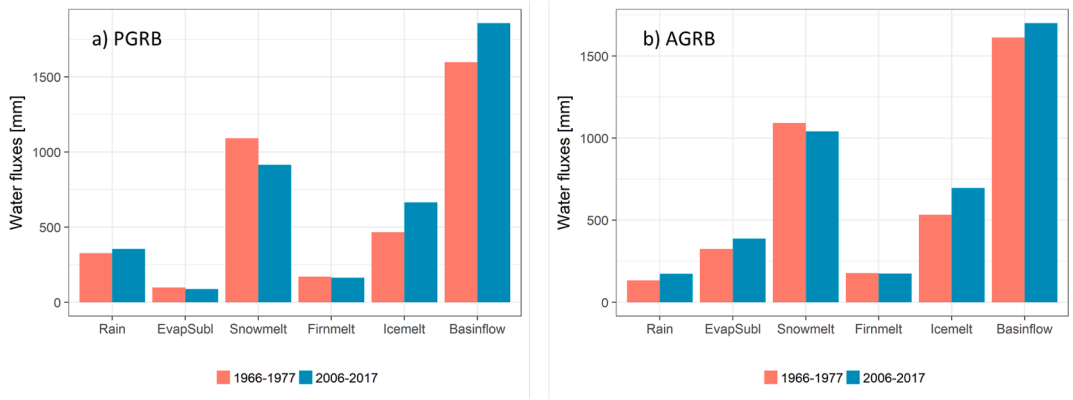

Fig. 18. Simulated annual water fluxes comparison between past (average of the period 1966–1977) and present (average of 2006–2017) periods for (a) PGRB and (b) AGRB. EvapSubl is the sum of all evaporation and sublimation processes from surfaces of snow, firn, ice and blowing snow.

Table 7
Annual water fluxes averaged over the periods of simulation.

Research basin	Water fluxes (mm)	Past (1966–1977)	Present (2006–2017)
PGRB	Rain (rainfall ratio)	325 (0.31)	354 (0.43)
	Precipitation	1435	1209
	Evaporation and sublimation	97	87
	Snow melt	1091	914
	Firn melt	170	162
	Ice melt	465	665
	Basin flow	1597	1857
	% flow from glacier firn/ice melt	38%	44%
AGRB	Rain (rainfall ratio)	132.3 (0.10)	173.0 (0.15)
	Precipitation	1433	1318
	Evaporation and sublimation	324	387
	Snow melt	1091	1040
	Firn melt	177	174
	Ice melt	532	696
	Basin flow	1612	1700
	% flow from glacier firn/ice melt	43%	50%

lakes, evolution of vegetation cover at the lower elevation of the basin, and evolution of drainage patterns were not considered in the model and its operation here. Debris-covered ice is becoming more common in Canadian mountain glaciers, particularly at the terminus. Currently, these areas are not treated distinctively, apart from assigning low albedo values. The debris cover may alter the surface energy balance due to the low thermal conductivity of debris (Vincent et al., 2016). The model also did not consider short-term impacts of meltwater refreezing to form superimposed ice on the glacier (Naz et al., 2014).

6. Conclusions

CRHM-glacier, a new, physically based, energy budget and mass balance, snow redistribution, spatially distributed glacier hydrology model was developed and applied to simulate both the glacier mass balance and streamflow of mountain glacierized basins. CRHM-glacier uses coupled mass and energy budgets, firnification and snow redistribution by wind and gravity to calculate snow melt, firn melt and ice melt separately, and it can be used in basins that are glacierized, partly glacierized, or glacier-free including basins undergoing transitional phases from glaciation to deglaciation. Hydrometeorological, streamflow and glaciological observations from the 1960 s to recent times at Peyto Glacier and new observations at Athabasca Glacier in the Canadian Rockies were used to quantify change, suggest model development, verify model operation, and drive models of glacier hydrology change. Bias-corrected reanalysis data and data from off-ice stations were used to drive the model, and on-glacier station observations were used to validate the model. When driven with locally measured off-ice meteorological data or bias-corrected reanalysis data and tested against specialized on-ice snow and ice surface height measurements, the model was able to simulate both accumulation and ablation of snow and ice quite well. The model was also able to simulate albedo and streamflow well without calibration of any parameters from observations. Model predictions of streamflow improved when processes describing snow redistribution by wind and gravity were included in the model, and model falsification showed that hydrological modelling must include a glacier component including firnification in order to successfully simulate the hydrology of glacierized basins. The validated model was used to simulate water balance and runoff components of both study basins for two time periods, past (1966–1977) and present (2006–2017). There was an increase in streamflow in the more recent period despite a marked decrease in precipitation and snow melt. This is due to increased glacier ice melt, which has become a larger runoff component during late summer. The increase in streamflow despite declining precipitation from these glaciers is a symptom of deglaciation and increased glacier ice melt since the 1960 s and is not sustainable into the future as these glaciers will disappear due to their persistently negative mass balances. The physical basis of this model and determination of physically identifiable model parameters from observations can reduce uncertainty in long-term simulations, especially those for future climates where calibrated parameters may no longer apply.

Author contributions

DP and JWP conceptualized the research. DP built the model and tested it at the research basins and prepared the manuscript. JWP contributed to model and methodology development, instrumented the glaciers and contributed to and revised the manuscript.

CRediT authorship contribution statement

Dhiraj Pradhananga: Conceptualization, Formal analysis, Investigation, Software, Writing – original draft. **John W. Pomeroy:** Conceptualization, Data curation, Funding acquisition, Software, Supervision, Writing – review & editing.

Declaration of Competing Interest

The authors declare that they have no known competing financial interests or personal relationships that could have appeared to influence the work reported in this paper.

Acknowledgments

The authors wish to acknowledge the decades of extremely challenging field research at Peyto and Athabasca glacier basins by dozens of scientists and students. Meriting special mention are Dr. D. Scott Munro (retired) of the University of Toronto and Michael N. Demuth (retired) of Natural Resources Canada whose legacy of research on Peyto Glacier including meteorological and mass balance observations made this study possible. Special mention also goes to the prescient scientists of the International Hydrological Decade who established Peyto Glacier as a research site, including Dr. Gordon Young of Environment Canada and Wilfrid Laurier University. Additional data was provided by Environment and Climate Change Canada's Meteorological Service of Canada and Water Survey of Canada, Parks Canada and Alberta Environment and Parks. Tom Brown and Xing Fang of the Centre for Hydrology supported CRHM development and operation/parameterization, respectively. Nammy Hang Kirat of The Small Earth Nepal supported GIS map production. Funding for this study was provided by the Canada Research Chairs, Canada Foundation for Innovation, Natural Sciences and Engineering Research Council of Canada through its Discovery Grants and the Changing Cold Regions Network, Alberta Innovation, and the Canada First Research Excellence Fund's Global Water Futures Programme. Special thanks go to the two anonymous reviewers for their careful and critical review of the manuscript and their several insightful comments and constructive suggestions, which helped to improve the manuscript.

References

Anderson, B., Lawson, W., Owens, I.F., Goodsell, B., 2006. Past and future mass balance of "Ka Roimata o Hine Hukatere" Franz Josef Glacier, New Zealand. J. Glaciol. 52, 597–607. https://doi.org/10.3189/172756506781828449.

Anderson, D.L.L., Benson, C.S.S., 1963. The densification and diagenesis of snow, in: Ice and Snow: Properties, Processes and Applications Properties, Processes and Applications. MIT Press, Cambridge, MA, pp. 391–411.

Arendt, A., Echelmeyer, K., Harrison, W., Lingle, C., Valentine, V.B., 2002. Rapid wastage of Alaska glaciers and their contribution to rising sea level. Science 297, 382–386. https://doi.org/10.1126/science.1072497.

Arendt, A., Walsh, J., Harrison, W., 2009. Changes of glaciers and climate in northwestern North America during the late twentieth century. J. Clim. 22, 4117–4134. https://doi.org/10.1175/2009JCLI2784.1.

Ayala Ramos, A.I., 2017. The role of surface sublimation in the summer mass balance of glaciers in the subtropical semiarid Andes. ETH Zurich. https://doi.org/10.3929/ETHZ-B-000000218.

Bakke, J., Nesje, A., 2011. Equilibrium-Line Altitude (ELA). In: Singh, V.P., Singh, P., Haritashya, U.K. (Eds.), Encyclopedia of Snow, Ice and Glaciers. Springer, Netherlands, Dordrecht, pp. 268–277. https://doi.org/10.1007/978-90-481-2642-2_140.

Barry, R.G., 2006. The status of research on glaciers and global glacier recession: a review. Prog. Phys. Geogr. 30, 285–306. https://doi.org/10.1191/0309133306pp478ra.

Bernhardt, M., Schulz, K., 2010. SnowSlide: A simple routine for calculating gravitational snow transport. Geophys. Res. Lett. 37 (11), 1–6. https://doi.org/10.1029/2010GL043086.

Berthier, E., 2004. Recent rapid thinning of the "Mer de Glace" glacier derived from satellite optical images. Geophys. Res. Lett. 31, 2–5. https://doi.org/10.1029/2004GL020706.

Berthier, E., Schiefer, E., Clarke, G.K.C., Menounos, B., Rémy, F., 2010. Contribution of Alaskan glaciers to sea-level rise derived from satellite imagery. Nat. Geosci. 3, 92–95. https://doi.org/10.1038/ngeo737.

Bertoncini, A., Aubry-Wake, D., Pomeroy, J.W., n.d. Large Area High-Resolution Albedo Retrievals from Remote Sensing to Assess the Impact of Wildfire Soot Deposition on High Mountain Snow and Ice Melt.

Bintanja, R., 2001. Snowdrift Sublimation in a Katabatic Wind Region of the Antarctic Ice Sheet. J. Appl. Meteorol. 40, 1952–1966. https://doi.org/10.1175/1520-0450(2001)040<1952:SSIAKW>2.0.CO;2.

Bintanja, R., Reijmer, C.H., 2001. A simple parameterization for snowdrift sublimation. J. Geophys. Res. 106, 31739–31748. https://doi.org/10.1029/2000JD000107.

Bojanowski, J.S., 2016. sirad: functions for calculating daily solar radiation and evapotranspiration. R package version 2.3-3.

Bravo, C., Loriaux, T., Rivera, A., Brock, B.W., 2017. Assessing glacier melt contribution to streamflow at Universidad Glacier, central Andes of Chile. Hydrol. Earth Syst. Sci. 21, 3249–3266. https://doi.org/10.5194/hess-21-3249-2017.

Brutsaert, W., 1982. Evaporation into the Atmosphere. D. Reidel, Dordrecht.

Chow, V.T., 1959. Open Channel Hydraulics. McGraw-Hill Inc, New York.

Clark, C.O., 1945. Storage and the unit hydrograph. Proc. Am. Soc. Civ. Eng. 69, 1419–1447.

Clarke, G.K.C.C., Berthier, E., Schoof, C.G., Jarosch, A.H., 2009. Neural networks applied to estimating subglacial topography and glacier volume. J. Clim. 22, 2146–2160. https://doi.org/10.1175/2008JCLI2572.1.

Collins, D.N., 1982. Flow-routing of meltwater in an alpine glacier as indicated by dye tracer tests. Bern, Beitrage zur Geol. der Schweiz—Hydrologie 28, 523–536.

Comeau, L.E.L., Pietroniro, A., Demuth, M.N., 2009. Glacier contribution to the North and South Saskatchewan Rivers. Hydrological Processes. 2640–2653. https://doi.org/10.1002/hyp.7409.

Dahal, P., Shrestha, M.L., Panthi, J., Pradhananga, D., 2020. Modeling the future impacts of climate change on water availability in the Karnali River Basin of Nepal Himalaya. Environ. Res. 185, 109430 https://doi.org/10.1016/j.envres.2020.109430.

de Woul, M., Hock, R., Braun, M., Thorsteinsson, T., Jóhannesson, T., Halldórsdóttir, S., 2006. Firn layer impact on glacial runoff: a case study at Hofsjökull. Iceland. Hydrol. Process. 20, 2171–2185. https://doi.org/10.1002/hyp.6201.

DeBeer, C.M., Sharp, M.J., Beer, C.M.D.E., Sharp, M.J., 2007. Recent changes in glacier area and volume within the southern Canadian Cordillera. Ann. Glaciol. 46, 215–221. https://doi.org/10.3189/172756407782871710.

Dee, D.P., Uppala, S.M., Simmons, A.J., Berrisford, P., Poli, P., Kobayashi, S., Andrae, U., Balmaseda, M.A., Balsamo, G., Bauer, P., Bechtold, P., Beljaars, A.C.M., van de Berg, L., Bidlot, J., Bormann, N., Delsol, C., Dragani, R., Fuentes, M., Geer, A.J., Haimberger, L., Healy, S.B., Hersbach, H., Hólm, E.V., Isaksen, L., Kållberg, P., Köhler, M., Matricardi, M., Mcnally, A.P., Monge-Sanz, B.M., Morcrette, J.J., Park, B. K., Peubey, C., de Rosnay, P., Tavolato, C., Thépaut, J.N., Vitart, F., 2011. The ERA-Interim reanalysis: Configuration and performance of the data assimilation system. Q. J. R. Meteorol. Soc. 137, 553–597. https://doi.org/10.1002/qj.828.

Demuth, M.N., Hopkinson, C., 2013. Glacier elevation data derived from Airborne Laser Terrain Mapper surveys over the reference monitoring glaciers of the Canadian Western and Northern Cordillera, August, 2006. Geological Survey of Canada and the Canadian Consortium for LiDAR Environmental, State and Evolution of Canada's Glaciers/ESS Climate Change Geoscience Programme Spatially Referenced Dataset, ESRI 3D ASCII files on archival hard drive.

Demuth, M.N., Keller, R., 2006. An assessment of the mass balance of Peyto glacier (1966–1995) and its relation to Recent and past-century climatic variability. In: Demuth, M.N., Munro, D.S., Young, G.J. (Eds.), Peyto Glacier: One Century of Science. National Hydrology Research Institute, Saskatoon, Saskatchewan, pp. 83–132.

Demuth, M.N., Munro, D.S., Young, G.J. (Eds.), 2006. Peyto Glacier: one century of science. National Hydrology Research Institute, Saskatoon, Saskatchewan.

Demuth, M.N., Pietroniro, A., 2003. The impact of climate change on the glaciers of the Canadian Rocky Mountain eastern slopes and implications for water resource-related adaptation in the Canadian prairies "Phase I " - Headwaters of the North Saskatchewan River Basin, PARC Project P55.

Derikx, L., 1975. The heat balance and associated runoff from an experimental site on a glacier tongue. Snow Ice-Symposium-Neiges Glaces (Proceedings Moscow Symp. August 1971; Actes du Colloq. Moscou, août 1971, 59–69.

Déry, S.J., Clifton, A., MacLeod, S., Beedle, M.J., 2010. Blowing Snow Fluxes in the Cariboo Mountains of British Columbia, Canada. Arctic. Antarct. Alp. Res. 42, 188–197. https://doi.org/10.1657/1938-4246-42.2.188.

Déry, S.J., Crow, W.T., Stieglitz, M., Wood, E.F., Dery, S., Crow, W.T., Stieglitz, M., Wood, E.F., 2004. Modeling Snow-Cover Heterogeneity over Complex Arctic Terrain for Regional and Global Climate Models*. J. Hydrometeorol. 5, 33–48. https://doi.org/10.1175/1525-7541(2004)005<0033:MSHOCA>2.0.CO;2.

Diolaiuti, G.A., Maragno, D., D'Agata, C., Smiraglia, C., Bocchiola, D., 2011. Glacier retreat and climate change: Documenting the last 50 years of Alpine glacier history from area and geometry changes of Dosde Piazzi glaciers (Lombardy Alps, Italy). Prog. Phys. Geogr. 35, 161–182. https://doi.org/10.1177/0309133311399494.

Doorschot, J., Raderschall, N., Lehning, M., 2001. Measurements and one-dimensional model calculations of snow transport over a mountain ridge. Ann. Glaciol. 32, 153–158.

Dornes, P.F., Pomeroy, J.W., Pietroniro, A., Carey, S.K., Quinton, W.L., 2008. Influence of landscape aggregation in modelling snow-cover ablation and snowmelt runoff in a sub-arctic mountainous environment. Hydrol. Sci. J. 53, 725–740. https://doi.org/10.1623/hysj.53.4.725.

Ellis, C.R., Pomeroy, J.W., Brown, T., MacDonald, J., 2010. Simulation of snow accumulation and melt in needleleaf forest environments. Hydrol. Earth Syst. Sci. 14, 925–940. https://doi.org/10.5194/hess-14-925-2010.

Engelhardt, M., Schuler, T.V., Andreassen, L.M., 2014. Contribution of snow and glacier melt to discharge for highly glacierised catchments in Norway. Hydrol. Earth Syst. Sci. 18, 511–523. https://doi.org/10.5194/hess-18-511-2014.

Essery, R., Etchevers, P., 2004. Parameter sensitivity in simulations of snowmelt. J. Geophys. Res. 109, 1–15. https://doi.org/10.1029/2004JD005036.

Essery, R., Pomeroy, J., 2004. Vegetation and topographic control of wind-blown snow distributions in distributed and aggregated simulations for an Arctic tundra basin. J. Hydrometeorol. 5, 735–744. https://doi.org/10.1175/1525-7541(2004)005<0735:VATCOW>2.0.CO;2.

Fang, X., Pomeroy, J.W., 2007. Snowmelt runoff sensitivity analysis to drought on the Canadian prairies. Hydrol. Process. 21, 2594–2609. https://doi.org/10.1002/hyp.6796.

Fang, X., Pomeroy, J.W., Ellis, C.R., MacDonald, M.K., DeBeer, C.M., Brown, T., 2013. Multi-variable evaluation of hydrological model predictions for a headwater basin in the Canadian Rocky Mountains. Hydrol. Earth Syst. Sci. 17, 1635–1659. https://doi.org/10.5194/hess-17-1635-2013.

Fang, X., Pomeroy, J.W., Westbrook, C.J., Guo, X., Minke, A.G., Brown, T., 2010. Prediction of snowmelt derived streamflow in a wetland dominated prairie basin. Hydrol. Earth Syst. Sci. 14, 991–1006. https://doi.org/10.5194/hess-14-991-2010.

Finger, D., Hugentobler, a., Huss, M., Voinesco, A., Wernli, H., Fischer, D., Weber, E., Jeannin, P.-Y.Y., Kauzlaric, M., Wirz, A., Vennemann, T., Hüsler, F., Schädler, B., Weingartner, R., H??sler, F., Sch??dler, B., Weingartner, R., Hüsler, F., Schädler, B., Weingartner, R., 2013. Identification of glacial meltwater runoff in a karstic environment and its implication for present and future water availability. Hydrol. Earth Syst. Sci. 17, 3261–3277. 10.5194/hess-17-3261-2013.

Fujita, K., Nuimura, T., 2011. Spatially heterogeneous wastage of Himalayan glaciers. Proc. Natl. Acad. Sci. 108, 14011–14014. https://doi.org/10.1073/pnas.1106242108.

Gallée, H., Trouvilliez, A., Agosta, C., Genthon, C., Favier, V., Naaim-Bouvet, F., 2012. Transport of Snow by the Wind: A Comparison Between Observations in Adélie Land, Antarctica, and Simulations Made with the Regional Climate Model MAR. Boundary-Layer Meteorol. 146, 133–147. https://doi.org/10.1007/s10546-012-9764-z.

Garen, D.C., Marks, D., 2005. Spatially distributed energy balance snowmelt modelling in a mountainous river basin: Estimation of meteorological inputs and verification of model results. J. Hydrol. 315, 126–153. https://doi.org/10.1016/j.jhydrol.2005.03.026.

Giesen, R.H., Oerlemans, J., 2012. Calibration of a surface mass balance model for global-scale applications. Cryosph. 6, 1463–1481. https://doi.org/10.5194/tc-6-1463-2012.

Goodison, B., 1972. An Analysis of Climate and Runoff Events for Peyto Glacier, Alberta, Inland Waters Directorate, Scientific Series No. 21. Environment Canada, Ottawa, Canada.

Granger, R.J., Gray, D.M., 1989. Evaporation from natural nonsaturated surfaces. J. Hydrol. 111, 21–29. https://doi.org/10.1016/0022-1694(89)90249-7.

Granger, R.J., Pomeroy, J.W., 1997. Sustainability of the western Canadian boreal forest under changing hydrological conditions. II. Summer energy and water use, in: Rosjberg, D., Boutayeb, N., Gustard, A., Kundzewicz, Z., Rasmussen, P. (Eds.), Sustainability of Water Resources under Increasing Uncertainty. IAHS Publ. No. 240, pp. 243–249.

Gray, D.M., Landine, P.G., 1988. An energy-budget snowmelt model for the Canadian Prairies. Can. J. Earth Sci. 25, 1292–1303. https://doi.org/10.1139/e88-124.

Gudmundsson, L., 2016. qmap: Statistical transformations for post-processing climate model output. R package version 1.0-4. R Packag. version 1.0-4.

Haeberli, W., Hoelzle, M., Paul, F., Zemp, M., Zu, C., 2007. Integrated monitoring of mountain glaciers as key indicators of global climate change : the European Alps. Ann. Glaciol. 46, 150–160.

Hannah, D.M., Gurnell, A.M., 2001. A conceptual, linear reservoir runoff model to investigate melt season changes in cirque glacier hydrology. J. Hydrol. 246, 123–141. https://doi.org/10.1016/S0022-1694(01)00364-X.

Herron, B.M.M., Langway, C.C., 1980. Firn densification: an empirical model. J. Glaciol. 25, 373–385.

Hock, R., 2005. Glacier melt: a review of processes and their modelling. Prog. Phys. Geogr. 29, 362–391. https://doi.org/10.1191/0309133305 pp453ra.

Hock, R., 2003. Temperature index melt modelling in mountain areas. J. Hydrol. 282, 104–115. https://doi.org/10.1016/S0022-1694(03)00257-9.

Hock, R., 1999. A distributed temperature-index ice- and snowmelt model including potential direct solar radiation. J. Glaciol. 45, 101–111.

Hock, R., Holmgren, B., 2005. A distributed surface energy-balance model for complex topography and its application to Storglaciaren. Sweden. J. Glaciol. 51, 25–36.

Hopkinson, C., Chasmer, L., Munro, S., Demuth, M.N., 2010. The influence of DEM resolution on simulated solar radiation-induced glacier melt. Hydrol. Process. 24, 775–788. https://doi.org/10.1002/hyp.7531.

Huss, M., 2011. Present and future contribution of glacier storage change to runoff from macroscale drainage basins in Europe. Water Resour. Res. 47, 1–14. https://doi.org/10.1029/2010WR010299.

Huss, M., Huss, M., Farinotti, D., Farinotti, D., Bauder, A., Bauder, A., Funk, M., Funk, M., 2005. Modelling runoff from highly glacierized alpine drainage basins in a changing climate. Hydrol. Process. 22, 1–14. https://doi.org/10.1002/hyp.7055.

Immerzeel, W.W., van Beek, L.P.H., Bierkens, M.F.P., 2010. Climate Change Will Affect the Asian Water Towers. Science (80-.) 328, 1382–1385. https://doi.org/10.1126/science.1183188.

Immerzeel, W.W., van Beek, L.P.H.H., Konz, M., Shrestha, A.B., Bierkens, M.F.P.P., 2012. Hydrological response to climate change in a glacierized catchment in the Himalayas. Clim. Change 110, 721–736. https://doi.org/10.1007/s10584-011-0143-4.

IPCC, 2007. Working Group II: Impacts, Adaptation and Vulnerability, IPCC Fourth Assessment Report: Climate Change.

Jansson, P., Hock, R., Schneider, T., 2003. The concept of glacier storage: a review. J. Hydrol. 282, 116–129. https://doi.org/10.1016/S0022-1694(03)00258-0.

Johnson, P.G., Power, J.M., 1985. Flood and landslide events, Peyto Glacier terminus, Alberta, Canada, 11–14 July 1983. J. Glaciol. 31, 86–91.

Kaser, G., Hardy, D.R., Mölg, T., Bradley, R.S., Hyera, T.M., Molg, T., Bradley, R.S., Hyera, T.M., 2004. Modern glacier retreat on Kilimanjaro as evidence of climate change: observations and facts. Int. J. Climatol. 24, 329–339. https://doi.org/10.1002/joc.1008.

Kaser, G., Juen, I., Georges, C., Gómez, J., Tamayo, W., 2003. The impact of glaciers on the runoff and the reconstruction of mass balance history from hydrological data in the tropical Cordillera Bianca. Perú. J. Hydrol. 282, 130–144. https://doi.org/10.1016/S0022-1694(03)00259-2.

Kehrl, L.M., Hawley, R.L., Osterberg, E.C., Winski, D.A., Lee, A.P., 2014. Volume loss from lower Peyto Glacier, Alberta, Canada, between 1966 and 2010. J. Glaciol. 60, 51–56. https://doi.org/10.3189/2014JoG13J039.

Kienzle, S.W., Nemeth, M.W., Byrne, J.M., Macdonald, R.J., 2012. Simulating the hydrological impacts of climate change in the upper North Saskatchewan River basin, Alberta. Canada. J. Hydrol. 412–413, 76–89. https://doi.org/10.1016/j.jhydrol.2011.01.058.

Klok, E.J.J.L., Oerlemans, J., Box, P.O., Utrecht, C.C., Klok, E.J.J.L., Oerlemans, J., 2002. Model study of the spatial distribution of the energy and mass balance of Morteratschgletscher. Switzerland. J. Glaciol. 48, 505–518. https://doi.org/10.3189/172756502781831133.

Krogh, S.A., Pomeroy, J.W., 2018. Recent changes to the hydrological cycle of an Arctic basin at the tundra-taiga transition. Hydrol. Earth Syst. Sci. 22, 3993–4014. https://doi.org/10.5194/hess-22-3993-2018.

Krogh, S.A., Pomeroy, J.W., Marsh, P., 2017. Diagnosis of the hydrology of a small Arctic basin at the tundra-taiga transition using a physically based hydrological model. J. Hydrol. 550, 685–703. https://doi.org/10.1016/j.jhydrol.2017.05.042.

Krogh, S.A., Pomeroy, J.W., McPhee, J., 2015. Physically Based Mountain Hydrological Modeling Using Reanalysis Data in Patagonia. J. Hydrometeorol. 16, 172–193. https://doi.org/10.1175/JHM-D-13-0178.1.

Leavesley, G., Lichty, R., Troutman, B., Saindon, L., 1983. Precipitation-runoff modelling system: user's manual. USGS, Water Resources Investigations Report 83–4238.

Li, H., Beldring, S., Xu, C.-Y., Huss, M., Melvold, K., Jain, S.K., 2015. Integrating a glacier retreat model into a hydrological model – Case studies of three glacierised catchments in Norway and Himalayan region. J. Hydrol. 527, 656–667. https://doi.org/10.1016/j.jhydrol.2015.05.017.

Liston, G.E., Elder, K., 2006. A Distributed Snow-Evolution Modeling System (SnowModel). J. Hydrometeorol. 7, 1259–1276. https://doi.org/10.1175/JHM548.1.

Liston, G.E., Hiemstra, C.A., 2011. The Changing Cryosphere: Pan-Arctic Snow Trends (1979–2009). J. Clim. 24, 5691–5712. https://doi.org/10.1175/JCLI-D-11-00081.1.

López-Moreno, J.I., Pomeroy, J.W., Alonso-González, E., Morán-Tejeda, E., Revuelto, J., 2020. Decoupling of warming mountain snowpacks from hydrological regimes. Environ. Res. Lett. 15 https://doi.org/10.1088/1748-9326/abb55f.

López-Moreno, J.I., Revuelto, J., Gilaberte, M., Morán-Tejeda, E., Pons, M., Jover, E., Esteban, P., García, C., Pomeroy, J.W., 2013. The effect of slope aspect on the response of snowpack to climate warming in the Pyrenees. Theor. Appl. Climatol. 117, 207–219. https://doi.org/10.1007/s00704-013-0991-0.

Luo, Y., Arnold, J., Liu, S., Wang, X., Chen, X., 2013. Inclusion of glacier processes for distributed hydrological modeling at basin scale with application to a watershed in Tianshan Mountains, northwest China. J. Hydrol. 477, 72–85. https://doi.org/10.1016/j.jhydrol.2012.11.005.

Lv, Z., Pomeroy, J.W., 2019. Detecting intercepted snow on mountain needleleaf forest canopies using satellite remote sensing. Remote Sens. Environ. 231, 111222 https://doi.org/10.1016/J.RSE.2019.111222.

MacDonald, M.K., Pomeroy, J.W., Pietroniro, A., 2010. On the importance of sublimation to an alpine snow mass balance in the Canadian Rocky Mountains. Hydrol. Earth Syst. Sci. 14, 1401–1415. https://doi.org/10.5194/hess-14-1401-2010.

MacDonald, M.K., Pomeroy, J.W., Pietroniro, A., 2009. Parameterizing redistribution and sublimation of blowing snow for hydrological models: tests in a mountainous subarctic catchment. Hydrol. Process. 23, 2570–2583. https://doi.org/10.1002/hyp.7356.

Magnusson, J., Farinotti, D., Jonas, T., Bavay, M., 2011. Quantitative evaluation of different hydrological modelling approaches in a partly glacierized Swiss watershed. Hydrol. Process. 2084, 2071–2084. https://doi.org/10.1002/hyp.7958.

Magnusson, J., Jonas, T., Lopez-Moreno, I., Lehning, M., 2010. Snow cover response to climate change in a high alpine and half-glacierized basin in Switzerland. Hydrol. Res. 41, 230–240. https://doi.org/10.2166/nh.2010.115.

Malecki, J., 2015. Snow Accumulation on a Small High-Arctic Glacier Svenbreen: Variability and Topographic Controls. Geogr. Ann. Ser. A Phys. Geogr. 97, 809–817. https://doi.org/10.1111/geoa.12115.

Marks, D., Domingo, J., Susong, D., Link, T., Garen, D., 1999. A spatially distributed energy balance snowmelt model for application in mountain basins. Hydrol. Process. 13, 1935–1959. https://doi.org/10.1002/(SICI)1099-1085(199909)13:12/13<1935::AID-HYP868>3.0.CO;2-C.

Marks, D., Dozier, J., 1992. Climate and energy exchange at the snow surface in the alpine region of the Sierra Nevada. Water Resour. Res. 28, 3043–3054.

Marks, D., Kimball, J., Tingey, D., Link, T., 1998. The sensitivity of snowmelt processes to climate conditions and forest cover during rain-on-snow: a case study of the 1996 Pacific Northwest flood. Hydrol. Process. 12, 1569–1587. https://doi.org/10.3189/172756401781819751.

Marsh, C.B., Pomeroy, J.W., Spiteri, R.J., 2012. Implications of mountain shading on calculating energy for snowmelt using unstructured triangular meshes. Hydrol. Process. 26, 1767–1778. https://doi.org/10.1002/hyp.9329.

Mauricio, Z.-B., 2014. hydroGOF: Goodness-of-fit functions for comparison of simulated and observed hydrological time series. https://doi.org/10.5281/zenodo.839854, R package version 0.4-0. https://cran.r-project.org/package=hydroGOF.

Meek, V., 1948. Glacier observations in the Canadian Cordillera. pp. 264-275. Retrieved from https://wgms.ch/downloads/published/former_data_reports/Meek_IAHS30_1948.pdf.

Mernild, S.H., Liston, G.E., Hasholt, B., 2007. Snow-distribution and melt modelling for glaciers in Zackenberg river drainage basin, north-eastern Greenland. Hydrol. Process. 21, 3249–3263. https://doi.org/10.1002/hyp.6500.

Mernild, S.H., Liston, G.E., Kane, D.L., Knudsen, N.T., Hasholt, B., 2008. Snow, runoff, and mass balance modeling for the entire Mittivakkat Glacier (1998–2006), Ammassalik Island, SE Greenland. Geogr. Tidsskr. J. Geogr. 108, 121–136. https://doi.org/10.1080/00167223.2008.10649578.

Michlmayr, G., Lehning, M., Koboltschnig, G., Holzmann, H., Zappa, M., Mott, R., Sch, W., 2008. Application of the Alpine 3D model for glacier mass balance and glacier runoff studies at Goldbergkees. Austria. Hydrol. Process. 22, 3941–3949. https://doi.org/10.1002/hyp.

Mo, R., Ye, C., Whitfield, P.H., 2014. Application Potential of Four Nontraditional Similarity Metrics in Hydrometeorology. J. Hydrometeorol. 15, 1862–1880. https://doi.org/10.1175/JHM-D-13-0140.1.
Moore, R.D., Demuth, M.N., 2001. Mass balance and streamflow variability at Place Glacier, Canada, in relation to recent climate fluctuations. Hydrol. Process. 15, 3473–3486. https://doi.org/10.1002/hyp.1030.
Moore, R.D., Fleming, S.W., Menounos, B., Wheate, R., Fountain, A., Stahl, K., Holm, K., Jakob, M., 2009. Glacier change in western North America : influences on hydrology, geomorphic hazards and water quality. Hydrol. Process. 23, 42–61. https://doi.org/10.1002/hyp.7162.
Mote, P.W., Hamlet, A.F., Clark, M.P., Lettenmaier, D.P., Mote, P.W., Hamlet, A.F., Clark, M.P., Lettenmaier, D.P., 2005. Declining Mountain Snowpack in Western North America*. Bull. Am. Meteorol. Soc. 86, 39–49. https://doi.org/10.1175/BAMS-86-1-39.
Mott, R., Lehning, M., Owe, H.L., Hynek, B., Michlmayer, G., Prokop, A., Oner, W.S.C.H., Faure, F., Lehning, M., Löwe, H., Hynek, B., Michlmayer, G., Prokop, A., Schöner, W., 2008. Simulation of seasonal snow-cover distribution for glacierized sites on Sonnblick, Austria, with the Alpine3D model. Ann. Glaciol. 49, 155–160. https://doi.org/10.3189/172756408787814924.
Munro, D.S., 2000. Progress in glacier hydrology : a Canadian perspective. Hydrol. Process. 14, 1627–1640.
Munro, D.S., 2004. Revisiting bulk heat transfer on Peyto Glacier, Alberta, Canada, in light of the OG parameterization. J. Glaciol. 50, 590–600. https://doi.org/10.3189/172756504781829819.
Munro, D.S., 2011a. Delays of supraglacial runoff from differently defined microbasin areas on the Peyto Glacier. Hydrol. Process. 25, 2983–2994. https://doi.org/10.1002/hyp.8124.
Munro, D.S., 2011b. Peyto Creek hydrometeorological database (Peyto Creek Base Camp AWS) [WWW Document]. IP3 Arch. URL www.usask.ca/ip3/data.
Munro, D.S., 2013. Creating a Runoff Record for an Ungauged Basin: Peyto Glacier, 2002-2007, in: Pomeroy, J.W., Spence, C., Whitfield, P.H. (Eds.), Putting Prediction in Ungauged Basins into Practice. Canadian Water Resources Association, pp. 197–204.
Munro, D.S., Marosz-Wantuch, M., 2009. Modeling Ablation on Place Glacier, British Columbia, from Glacier and Off-glacier Data Sets. Arctic. Antarct. Alp. Res. 41, 246–256. https://doi.org/10.1657/1938-4246-41.2.246.
Munro, D.S., Young, G.J., 1982. An Operational Net Shortwave Radiation Model for Glacier Basins. Water Resour. Res. 18, 220–230.
Nash, J.E., Sutcliffe, J.V., 1970. River flow forecasting through conceptual models part I - A discussion of principles. J. Hydrol. 10, 282–290. https://doi.org/10.1016/0022-1694(70)90255-6.
Naz, B.S., Frans, C.D., Clarke, G.K.C., Burns, P., Lettenmaier, D.P., 2014. Modeling the effect of glacier recession on streamflow response using a coupled glacio-hydrological model. Hydrol. Earth Syst. Sci. 18, 787–802. https://doi.org/10.5194/hess-18-787-2014.
Oerlemans, J., 1991. A model for the surface balance of ice masses: part I. Alpine glaciers. Zeitschrift fur Gletscherkd. und Glazialgeol. 27 (28), 63–83.
Oerlemans, J., Knap, W.H., 1998. A 1 year record of global radiation and albedo in the ablation zone of Morteratschgletscher. Switzerland. J. Glaciol. 44, 231–238.
Oerter, H., Baker, D., Moser, H., Reinwarth, O., 1981. Glacial-hydrological investigations at the Vernagtferner Glacier as a basis for a discharge model. Nord. Hydrol. 12, 335–348.
Ohmura, A., 2006. Changes in mountain glaciers and ice caps during the 20th century. Ann. Glaciol. 43, 361–368. https://doi.org/10.3189/172756406781812212.
Ommanney, C.S.L., 2002. Glaciers of North America — Glaciers of Canada: Glaciers of the Canadian Rockies, in: Williams, R.S., Ferrigno, J.G. (Eds.), Satellite Image Atlas of Glaciers of the World. pp. J199–J289.
Ommanney, C.S.L., 1987. Peyto Glacier: A Compendium of Information Prepared for Parks Canada. Saskatoon, Saskatchewan, S7N 3H5.
Plüss, C., Ohmura, A., 1997. Longwave radiation on snow-covered mountainous surfaces. J. Appl. Meteorol. 36, 818–824. https://doi.org/10.1175/1520-0450-36.6.818.
Pomeroy, J.W., 1989. A process-based model of snow drifting. Ann. Glaciol. 13, 237–240.
Pomeroy, J.W., Fang, X., Shook, K., Whitfield, P.H., 2013. Predicting in ungauged basins using physical principles obtained using the deductive, inductive, and abductive reasoning approach, in: Pomeroy, J.W., Spence, C., Whitfield, P.H. (Eds.), Putting Prediction in Ungauged Basins into Practice. Canadian Water Resources Association, pp. 41–62.
Pomeroy, J.W., Gray, D.M., Brown, T., Hedstrom, N.R., Quinton, W.L., Granger, R.J., Carey, S.K., 2007. The cold regions hydrological model: a platform for basing process representation and model structure on physical evidence. Hydrol. Process. 21, 2650–2667. https://doi.org/10.1002/hyp.6787.
Pomeroy, J.W., Gray, D.M., Landline, P.G., 1993. The Prairie Blowing Snow Model: characteristics, validation, operation. J. Hydrol. 144, 165–192. https://doi.org/10.1016/0022-1694(93)90171-5.
Pomeroy, J.W., Gray, D.M., Shook, K.R., Toth, B., Essery, R.L.H., Pietroniro, A., Hedstrom, N., 1998a. An evaluation of snow accumulation and ablation processes for land surface modelling. Hydrol. Process. 12, 2339–2367. https://doi.org/10.1002/(SICI)1099-1085(199812)12:15<2339::AID-HYP800>3.0.CO;2-L.
Pomeroy, J.W., Li, L., 2000. Prairie and arctic areal snow cover mass balance using a blowing snow model. J. Geophys. Res. 105, 26619–26634. https://doi.org/10.1029/2000JD900149.
Pomeroy, J.W., Parviainen, J., Hedstrom, N., Gray, D.M., 1998b. Coupled modelling of forest snow interception and sublimation. Hydrol. Process. 12, 2317–2337. https://doi.org/10.1002/(SICI)1099-1085(199812)12:15<2317::AID-HYP799>3.0.CO;2-X.
Poulin, A., Brissette, F., Leconte, R., Arsenault, R., Malo, J., 2011. Uncertainty of hydrological modelling in climate change impact studies in a Canadian, snow-dominated river basin. J. Hydrol. 409, 626–636. https://doi.org/10.1016/j.jhydrol.2011.08.057.
Pradhananga, D., Pomeroy, J., Aubry-Wake, C., Munro, D.S., Shea, J., Demuth, M., Kirat, N.H., Menounos, B., Mukherjee, K., 2021. Hydrometeorological, glaciological and geospatial research data from the Peyto Glacier Research Basin in the Canadian Rockies. Earth Syst. Sci. Data 13, 2875–2894. https://doi.org/10.5194/essd-13-2875-2021.
Priestley, C.H.B., Taylor, R.J., 1972. On the Assessment of Surface Heat Flux and Evaporation Using Large-Scale Parameters. Mon. Weather Rev. 100, 81–92. https://doi.org/10.1175/1520-0493(1972)100<0081:otaosh>2.3.co;2.
R Core Team, 2017. R: A language and environment for statistical computing. R Foundation for Statistical Computing. https://www.r-project.org/.
Radić, V., Hock, R., 2011. Regionally differentiated contribution of mountain glaciers and ice caps to future sea-level rise. Nat. Geosci. 4, 91–94. https://doi.org/10.1038/ngeo1052.
Rasouli, K., Pomeroy, J.W., Janowicz, J.R., Carey, S.K., Williams, T.J., 2014. Hydrological sensitivity of a northern mountain basin to climate change. Hydrol. Process. 28, 4191–4208. https://doi.org/10.1002/hyp.10244.
Reynolds, J.R., Young, G.J., 1997. Changes in areal extent, elevation and volume of Athabasca Glacier, Alberta, Canada, as estimated from a series of maps produced between 1919 and 1979. Ann. Glaciol. 24, 60–65.
Rood, S., Pan, J., Gill, K., Franks, C., Samuelson, G., Shepherd, A., 2008. Declining summer flows of Rocky Mountain rivers: Changing seasonal hydrology and probable impacts on floodplain forests. J. Hydrol. 349, 397–410. https://doi.org/10.1016/j.jhydrol.2007.11.012.
RStudio, 2017. RStudio: Integrated development environment for R (Version 1.0.143). http://www.rstudio.org/.
Schiefer, E., Menounos, B., Wheate, R., 2007. Recent volume loss of British Columbian glaciers, Canada. Geophys. Res. Lett. 34, 1–6. https://doi.org/10.1029/2007GL030780.
Sedgwick, J.K., Henoch, W.E.S., 1975. 1966 Peyto Glacier Map, Banff National Park, Alberta. Environment Canada, IWD 1010, 1:10,000.
Shannon, S., Smith, R., Wiltshire, A., Payne, T., Huss, M., Betts, R., Koutroulis, A., Jones, D., Harrison, S., 2019. Global glacier volume projections under high-end climate change scenarios. Cryosph. 13, 325–350. https://doi.org/10.5194/tc-13-325-2019.
Shea, J.M., Immerzeel, W.W., Wagnon, P., Vincent, C., Bajracharya, S., 2015. Modelling glacier change in the Everest region, Nepal Himalaya. Cryosph. 9, 1105–1128. https://doi.org/10.5194/tc-9-1105-2015.
Shea, J.M., Marshall, S.J., 2007. Atmospheric flow indices, regional climate, and glacier mass balance in the Canadian Rocky Mountains. Int. J. Climatol. 27, 233–247. https://doi.org/10.1002/joc.1398.
Shook, K.. MSCr: Downloads daily and hourly MSC data from the webserver. Reads in monthly, daily and hourly MSC data from files. https://citeseerx.ist.psu.edu/viewdoc/download?doi=10.1.1.723.1508&rep=rep1&type=pdf.
Shook, K., 2016a. CRHMr: pre- and post- processing for the Cold Regions Hydrological Modelling (CRHM) platform.
Shook, K., 2016b. Reanalysis: Creates Cold Regions Hydrological Modelling (CRHM) platform observations files from reanalysis data.
Shook, K., Pomeroy, J., 2011. Synthesis of incoming shortwave radiation for hydrological simulation. Hydrol. Res. 42, 433. https://doi.org/10.2166/nh.2011.074.
Sicart, J.E., Pomeroy, J.W., Essery, R.L.H., Bewley, D., 2006. Incoming longwave radiation to melting snow: observations, sensitivity and estimation in Northern environments. Hydrol. Process. 20, 3697–3708. https://doi.org/10.1002/hyp.6383.
Singh, P., Bengtsson, L., 2005. Impact of warmer climate on melt and evaporation for the rainfed, snowfed and glacierfed basins in the Himalayan region. J. Hydrol. 300, 140–154. https://doi.org/10.1016/j.jhydrol.2004.06.005.
Stahl, K., Moore, R.D., Shea, J.M., Hutchinson, D., Cannon, A.J., 2008. Coupled modelling of glacier and streamflow response to future climate scenarios. Water Resour. Res. 44, 1–13. https://doi.org/10.1029/2007WR005956.
Strasser, U., Bernhardt, M., Weber, M., Liston, G.E., Mauser, W., 2008. Is snow sublimation important in the alpine water balance? Cryosphere 2, 53–66. https://doi.org/10.5194/tc-2-53-2008.
Tennant, C., Menounos, B., 2013. Glacier change of the Columbia Icefield, Canadian Rocky Mountains, 1919–2009. J. Glaciol. 59, 671–686. https://doi.org/10.3189/2013JoG12J135.
Thiery, W., Gorodetskaya, I.V.V., Bintanja, R., van Lipzig, N.P.M.P.M., Van Den Broeke, M.R.R., Reijmer, C.H.H., Kuipers Munneke, P., 2012. Surface and snowdrift sublimation at Princess Elisabeth station, East Antarctica. Cryosph. 6, 841–857. https://doi.org/10.5194/tc-6-841-2012.
Uppala, S.M., KÅllberg, P.W., Simmons, A.J., Andrae, U., Bechtold, V.D.C., Fiorino, M., Gibson, J.K., Haseler, J., Hernandez, A., Kelly, G.A., Li, X., Onogi, K., Saarinen, S., Sokka, N., Allan, R.P., Andersson, E., Arpe, K., Balmaseda, M.A., Beljaars, A.C.M., Berg, L. Van De, Bidlot, J., Bormann, N., Caires, S., Chevallier, F., Dethof, A., Dragosavac, M., Fisher, M., Fuentes, M., Hagemann, S., Hólm, E., Hoskins, B.J., Isaksen, L., Janssen, P.A.E.M., Jenne, R., Mcnally, A.P., Mahfouf, J.-F., Morcrette, J.-J., Rayner, N.A., Saunders, R.W., Simon, P., Sterl, A., Trenberth, K.E., Untch, A., Vasiljevic, D., Viterbo, P., Woollen, J., 2005. The ERA-40 re-analysis. Q. J. R. Meteorol. Soc. 131, 2961–3012. 10.1256/qj.04.176.
Van Pelt, W., Kohler, J., 2015. Modelling the long-term mass balance and firn evolution of glaciers around Kongsfjorden. Svalbard. J. Glaciol. 61, 731–744. https://doi.org/10.3189/2015JoG14J223.

Verbunt, M., Gurtz, J., Jasper, K., Lang, H., Warmerdam, P., Zappa, M., 2003. The hydrological role of snow and glaciers in alpine river basins and their distributed modeling. J. Hydrol. 282, 36–55. https://doi.org/10.1016/S0022-1694(03)00251-8.

Verseghy, D.L., 1991. CLASS - A Canadian Land Surface Scheme for GCMS. I. Soil Model. Int. J. Climatol. 11, 111–133. https://doi.org/10.1002/joc.3370110202.

Vincent, C., Wagnon, P., Shea, J.M., Immerzel, W.W., Kraaijenbrink, P., Shrestha, D., Soruco, A., Arnaud, Y., Brun, F., Berthier, E., Sherpa, S.F., 2016. Reduced melt on debris-covered glaciers: investigations from Changri Nup Glacier. Nepal. Cryosph. 10, 1845–1858. https://doi.org/10.5194/tc-10-1845-2016.

Walmsley, J., Taylor, P., Salmon, J., 1989. Simple guidelines for estimating wind speed variations due to small-scale topographic features–an update. Clim. Bull 23, 3–14.

Walter, M.T., Brooks, E.S., McCool, D.K., King, L.G., Molnau, M., Boll, J., 2005. Process-based snowmelt modeling: does it require more input data than temperature-index modeling? J. Hydrol. 300, 65–75. https://doi.org/10.1016/j.jhydrol.2004.05.002.

Wang, Z., Bovik, A.C., 2002. A universal image quality index. Signal Process. Lett. IEEE 9, 81–84. https://doi.org/10.1109/97.995823.

Wayand, N.E., Marsh, C.B., Shea, J.M., Pomeroy, J.W., 2018. Globally scalable alpine snow metrics. Remote Sens. Environ. 213, 61–72. https://doi.org/10.1016/j.rse.2018.05.012.

WGMS, 2020. Fluctuations of Glaciers Database [WWW Document]. World Glacier Monit. Serv. Zurich, Switz. 10.5904/wgms-fog-2020-08.

Young, G.J., Stanley, A.D., 1976. Canadian Glaciers in the International Hydrological Decade Program, 1965-1974 No. 4. Peyto Glacier, Alberta - Summary of measurements.

Zemp, M., Frey, H., Gärtner-Roer, I., Nussbaumer, S.U., Hoelzle, M., Paul, F., Haeberli, W., Denzinger, F., Ahlstrøm, A.P., Anderson, B., Bajracharya, S., Baroni, C., Braun, L.N., Càceres, B.E., Casassa, G., Cobos, G., Dàvila, L.R., Delgado Granados, H., Demuth, M.N., Espizua, L., Fischer, A., Fujita, K., Gadek, B., Ghazanfar, A., Hagen, J. O., Holmlund, P., Karimi, N., Li, Z., Pelto, M., Pitte, P., Popovnin, V.V., Portocarrero, C.A., Prinz, R., Sangewar, C.V., Severskiy, I., Sigurdsson, O., Soruco, A., Usubaliev, R., Vincent, C., 2015. Historically unprecedented global glacier decline in the early 21st century. J. Glaciol. 61, 745–762. https://doi.org/10.3189/2015JoG15J017.

Zhou, J., Pomeroy, J.W., Zhang, W., Cheng, G., Wang, G., Chen, C., 2014. Simulating cold regions hydrological processes using a modular model in the west of China. J. Hydrol. 509, 13–24. https://doi.org/10.1016/j.jhydrol.2013.11.013.